

https://dspace.org/

Automatic control for a Hvdc transmission scheme

Francocci, Enrico

2015-01-21
http://hdl.handle.net/10539/16671

Downloaded from a DSpace repository. https://dspace.org/

AUTOMATIC CONTROL FOR A HVDC TRANSMISSION SCHEME

Enrico Francocci

A dissertation submitted to the Faculty of Engineering, University of Witwatersrand, Johannesburg, in fulfilment of the requirements for the degree of Master of Science in Electrical Engineering

Johannesburg, 1986

In memory of my father

Filippo Francocci

1905-1971

DECLARATION

I declare that this dissertation is my own, unaided work. It is being submitted for the Degree of Master of Science in Electrical Engineering at the University of the Witwatersrand, Johannesburg. It has not been submitted before for any degree or examination in any other University.

E. M Francois
(Signature of candidate)

19 day of February

ABSTRACT

This dissertation discusses and analyses a High Voltage Direct Current (HVDC) control system and its various functions, with particular reference to the Cahora Bassa-Apollo scheme. In this scheme, inverter operation is governed mainly by the control system at the inverter end which also regulates the power transmitted by the HVDC link in conjunction with the control system at the rectifier end.

An integrated and consistent approach is developed for analysing many aspects of HVDC transmission system behaviour. The author's experience with the working system is incorporated in this study. The dissertation attempts to contribute towards knowledge on the very important subject of HVDC automatic control, which plays a predominant role in HVDC transmission in general, the methods adopted to cope with problems inherent in this type of transmission, and the operations and processes performed by the automatic control equipment.

PREFACE

For several years the author was Escom's maintenance engineer at the Apollo inverter station (Irene, South Africa), which receives DC power from the Songo rectifier station - 1414 km north east of Apollo in Mocambique. The Songo-Apollo DC transmission system is part of the gigantic Cahora Bassa hydroelectric project.

The author was specifically involved in the maintenance of the control system at the inverter end, and in performing this task it was realised that although much published and unpublished material on HVDC schemes is available, there is insufficient literature specifically on HVDC control systems. Furthermore, most of the available documentation covers specific problems and studies performed by universities, and as such does not facilitate the understanding of the control processes of HVDC transmission, especially for those approaching this type of electrical engineering for the first time. There is a lack of literature on HVDC automatic control systems mainly because it was only a few decades ago that the use of HVDC began to be considered as a serious challenge to the established AC transmission systems. Moreover, many aspects of HVDC transmission behaviour are not very well known or documented, and certain investigations have not yet been finalised.

It was against this background that the author felt that a serious need for an integrated and consistent study of the automatic control aspects of HVDC transmission system existed.

ACKNOWLEDGEMENTS

I wish primarily to thank Escom, which provided the financial assistance for the realization of this dissertation.

I am obliged to Prof. I.M. MacLeod, of the Electrical Engineering Faculty of the University of Witwatersrand, Johannesburg, for his invaluable help and advice for the preparation of the dissertation.

I thank my colleagues of the Apollo Specialized Maintenance Section for their valuable assistance given to me.

CONTENTS

		PAGE
DECLARATION		ii
ABSTRACT		iii
PREFACE		iv
ACKNOWLEDGEMENTS		v
CONTENTS		vi
LIST OF FIGURES		xi
LIST OF TABLES		xvi
LIST OF SYMBOLS		xvii
1	INTRODUCTION	1
1.1	An Historical Review of DC Transmission	1
1.2	DC Application Considerations	2
1.3	Principles of DC Power Transfer	4
1.4	The Cahora Bassa-Apollo Scheme	7
1.5	Cahora Bassa Generating Plant	9
1.6	Songo-Apollo DC Transmission	9
1.7	Thyristor Valves Used at the Songo and Apollo Converter Stations	10
1.8	Outline of the Dissertation	12
	References	15
2	BASIC THEORY OF HIGH VOLTAGE DC TRANSMISSION SYSTEMS	16
2.1	Operating Modes of a DC Transmission System	16
2.2	Three-phase Converters	16
2.3	Rectification and Inversion in DC Transmission	19
2.4	Definition of the Firing Angles α and β, Overlap Angles μ_α, μ_γ and Extinction Angles δ and γ	23

CONTENTS

		PAGE
2.5	No-load Voltage and the Output Direct Voltage at the Converters	25
2.6	Direct Voltage Drops due to α and μ_α	27
2.7	The Secondary Current Wave Forms and the Power Flow through a Converter	28
2.8	Summary	36
	References	37
3	CONTROL ASPECTS OF HVDC SYSTEMS	39
3.1	Control Requirements of an HVDC System	39
3.2	Current and Voltage Control in HVDC Transmission	40
3.3	Converter Characteristics and Determination of DC Transmission Working Points	47
3.4	Voltage Drop at Rectifier Station - Current Control by the Inverter Real-Time Processor	53
3.5	Voltage Drops at the Inverter Station	56
3.6	Tap-changer Control at the Rectifier and Inverter Stations	58
3.7	Power Control	64
3.7.1	General	64
3.7.2	Master Power Controller at the Rectifier Substation	65
3.7.3	Control of Frequency on DC Load Rejection	68
3.8	Current Reference and Actual Current	69
3.8.1	Current Reference Limits and Permissible Rate of Change	69
3.8.2	Reduction of the Current Limits	74
3.9	Current Controller	75
3.9.1	Current and Voltage [illegible]lers at Rectifier Station	75
3.9.2	Current Control[illegible]ter Station	81

CONTENTS PAGE

3.10	Firing Pulse Spacing Control	81
	Summary	83
	References	83
4	THE INVERTER AND ITS AUTOMATIC CONTROL	85
4.1	Introduction	85
4.2	Real Time Processors at the Inverter Station	88
4.3	The Extinction Control Loop at Inverter Station	89
4.3.1	Indoors: General about the Error Function, Feed-back and Control Elements of the Extinction Controller	90
4.3.2	The γ-Controller and Error Functions	92
4.3.3	Generation and Sychronization of the Firing Pulses	102
4.3.4	The Firing Pulse and the By-pass Logic	106
4.3.5	Transducer (γ Control Loop Feed-back)	110
4.4	Open Control Loops and Firing Control Ranges	115
4.5	Firing Control During Transients: SON, NOSOF and FASOF	120
4.6	Outdoor Firing Control Circuits	123
4.6.1	Command Unit and Emergency Firing Pulses	123
4.6.2	Gate Pulse amplifier (by Zamco Documentation)	126
	Summary	131
	References	133
5	DC PROTECTION	135
5.1	Commutation Failure Protection	135
5.1.1	Definition of Commutation	135
5.1.2	Causes of the Commutation Failure	135
5.1.3	Commutation Failure in the Inverters	135
5.1.4	Circuit-commutated Recovery Time and Hold-off Interval (γ Extinction Angle)	136

CONTENTS PAGE

5.1.5	Consequent Commutation Failure in an Inverter	139
5.1.6	DC Terminals Short-circuited by the Occurrence of a Bridge Commutation Failure	139
5.1.7	Commutation Failure Protection at the Inverter Station	141
5.1.8	The Commutation Failure Detector Input Signals	147
5.1.9	Detector Operation: Intercept and set Pulses	143
5.1.10	Timer Units of the Commutation Failure Detector	148
5.1.11	Advance Firing Angle Setting and Idref=0,3 CMD to the Rectifier Station	148
5.1.12	Real and False Commutation [illegible]e	149
5.1.13	Multiple Commutation F[illegible] Integration FASOF (Fast switch off)	152
5.1.14	AC System Fault	156
5.2	DC Line Protection	156
5.2.1	Causes of Short-circuits on the DC Lines	156
5.2.2	Basic Principles of Line Protection Design	158
5.2.3	Travelling Waves on the DC Line	159
5.2.4	The Travelling Wave Protection Signal	161
5.2.5	Travelling Wave Detector at the Rectifier	161
5.2.6	Protective Shifting of Firing Angle at the Rectifier End	164
5.2.7	Travelling Wave Protection at the Inverter End	165
5.2.8	The Re-energization of a DC Line after Line Fault Occurrences	166
5.2.9	Protection and Re-energization at Songo Substation	167
5.2.10	Successful and Unsuccessful Reclosure Attempts	171

CONTENTS PAGE

5.3	Differential Protection	173
5.3.1	Differential Protection at the Rectifier and Inverter Stations	173
5.4	*Line Faults Affecting DC Power Transmission* on Bipolar and Monopolar Operation	178
5.5	Dynamic Responses at the Generating Plant and Control Systems for a 50% Load Rejection	189
5.6	Valve Protection	182
5.6.1	Valve Firing Monitoring	182
5.6.2	Differential and Overcurrent Protection	184
	Summary and Conclusion	187
	References	189
6	CONCLUSION	191
6.1	General	191
6.2	HVDC control and protection	192
6.3	Future directions	194

BIBLIOGRAPHY

LIST OF FIGURES

Figure		Page
1.1	Comparative costs of AC and DC transmission system	4
1.2	Detailed HVDC link	6
1.3	Simple DC link	6
1.4	The gorge of Cahora Bassa	8
1.5	Valve tanks forming a bridge	12
1.6	Thyristor stacks forming a valve, valve damping network and voltage grading network at Apollo	15
2.1	DC transmission operating mode	17
2.2a	Bridge converter	18
2.2b	Waves of instantaneous EMFs of AC source	18
2.3	Standard Graetz rectifier	20
2.4	Graetz rectifier waveform	20
2.5	DC voltage control by changing control angle	22
2.6	Rectification and inversion angles	24
2.7	Curves of μ_R (μ_I) plotted from equation 2.4.4 and 2.4.5	26
2.8	Modifiction due to AC reactance and gate control of DC voltage wave form and secondary current	26
2.9	Equivalent circuit of a converter during commutation	31
2.10	Curves plotted from equations 2.7.9 and 2.7.10	32
2.11	Relation between ignition delay and phase displacement	33
2.12	Instantaneous current and voltage of three-phase bridge convertor	34

Figure		Page
2.13	Wave forms of currents and voltages of three-phase bridge inverter	35
2.14	Wave forms of voltage across a valve	36
3.1	Schematic DC link representation	41
3.2	General automatic control block diagram of a DC transmission system	42
3.3	Basic automatic control for DC transmission	43
3.4	List of voltages current, and power values	45
3.5a	Rectifier characteristic	48
3.5b	Inverter characteristic	48
3.6	The classical characteristics	49
3.7	Line to line voltage replica and the advanced firing angle	51
3.8	Inverter oscillograms	55
3.9	Records of line voltage drop due to the loss of an inverter	59
3.10a	Variation of E_p and U_{di} with tap position (rectifier)	60
3.10b	Variation of AC system voltage with tap position (inverter)	61
3.11	Tap controller block diagram	63
3.12	Simplified schematic diagram of the Master Power Controller	67
3.13	Schematic block diagram of the generation and control of the reference currents	70

Figure		Page
3.14	Non linear operating characteristics of the device to influence the reference input of the current control circuit	72
3.15	Limitation of the rate of change of the reference current input at rectifier current controller by the slope limiter.	73
3.16	Block diagram of the current controller	78
3.17	Non linear characteristic of the current controller	79
3.18	Operating characteristic of the corrective variable $U_{\alpha t}$	80
4.1	Inverter bridge and DC/AC current conversion	86
4.2	Voltage across two inverter valves consecutively fired	87
4.3	Block diagram of the real time inverter processor	89
4.4	Extinction angle control loop	91
4.5	γ-controller block diagram	93
4.6	γ-controller-current controller threshold selector	96
4.7	γ control loop block diagram	97
4.8	Current controller controls firing	99
4.9	Control loop block diagram	100
4.10	Basic circuit diagram of the pulse generator	103
4.11	Time diagram of the pulse generator	103
4.12	Thyropulse or ring counter	105
4.13	Response of the pulse generator for $\xi_F = f(t)$	107
4.14	Pulse firing and by-pass logic	109

Figure		Page
3.14	Non linear operating characteristics of the device to influence the reference input of the current control circuit	72
3.15	Limitation of the rate of change of the reference current input at rectifier current controller by the slope limiter.	73
3.16	Block diagram of the current controller	78
3.17	Non linear characteristic of the current controller	79
3.18	Operating characteristic of the corrective variable U_{st}	80
4.1	Inverter bridge and DC/AC current conversion	86
4.2	Voltage across two inverter valves consecutively fired	87
4.3	Block diagram of the real time inverter processor	89
4.4	Extinction angle control loop	91
4.5	γ-controller block diagram	93
4.6	γ-controller-current controller threshold selector	96
4.7	γ control loop block diagram	97
4.8	Current controller controls firing	99
4.9	Control loop block diagram	100
4.10	Basic circuit diagram of the pulse generator	103
4.11	Time diagram of the pulse generator	103
4.12	Thyropulse or ring counter	105
4.13	Response of the pulse generator for $\xi_f = f(t)$	107
4.14	Pulse firing and by-pass logic	109

Figure		Page
4.15	Control loop feedback circuit	111
4.16	Forming γ actual value by collecting 6 extinction angles	112
4.17	Forming γ actual value for one valve	114
4.18	90° rate of change limiter	116
4.19	Voltage control and selective switches	118
4.20	Voltage control and inverter output voltage during transient	119
4.21	Valve firing during bridge switch-on	122
4.22	Command unit logic	125
4.23	Gate pulse amplifier as parallel-resonant cuit inverter	128
4.24	Voltage and current diagrams on the parallel-resonant circuit inverter of the gate pulse amplifier	130
4.25	Functional block diagram of the inverter indoor automatic control	132
5.1.1	Normal valve commutation	137
5.1.2	Valve commutation failure	138
5.1.3	Voltage grading network of Apollo valves	138
5.1.4	DC and AC short-circuit due to bridge valve commutation	140
5.1.5	Commutation failure detector	145

Figure		Page
5.1.6	Responses by a single dip below the rated extinction angle	146
5.1.7	Response by commutation failure	147
5.1.8	Set and intersept pulse firing	150
5.1.9	Back up Fasof and Idref = 0,3 IdN CMD logic circuit	151
5.1.10	False commutation failure oscillogrames	153
5.1.11	Multiple commutation failure time integrating circuit	154
5.1.12	Repetitive commutation failures due to a missing ignition pulse	155
5.1.13	AC system fault	157
5.2.1	Diagram of the travelling wave detection system	162
5.2.2	When t4 > tH the TW protection pulse is generated	164
5.2.3	Layout of the re-energization system at Songo	168
5.2.4	Sequence of events during four re-energization attempts	169
5.2.5	Line protection unsuccessful attempt	172
5.2.6	Successful re-energization attempt	174
5.3.1	Layout of the line difference protection	175
5.3.2	3-point controller to evaluate the difference between current at the extremities of DC link	177
5.5.1	Generating plant response for a 50% load rejection	181
5.5.2	AC frequency and imported power at the inverter end	183

LIST OF TABLES PAGE

Table 1 3

SYMBOLS FOR PHYSICAL QUANTITIES

α	firing delay angle (rectifier control angle)
β	firing advance angle (inverter control angle)
δ	extinction delay angle
γ	extinction advance angle
$\mathcal{E}f$	control voltage function
μ_α	overlap angle in rectifier commutation
μ_γ	overlap angle in inverter commutation
E_l	line to line voltage amplitude
E_m	line to ground voltage amplitude
E_p	AC system voltage (bridge transformer primary)
E_v	AC system voltage (bridge transformer secondary)
I_d	direct system current
I_{dact}	actual direct current
I_{dN}	direct current nominal value
I_{d1}	pole 1 direct current
I_{d2}	pole 2 direct current
I_{dref}	reference or control current
I_{ifo}	fundamental secondary current
P_t	DC power transmitted by rectifier
P_r	DC power received by the inverter
U_d	DC voltage at the converter output
U_{di}	converter EMF or converter internal voltage
$\omega(1\alpha)p$	power component correction factor
$\omega(1\alpha)r$	reactive component correction factor

SYMBOLS FOR PHYSICAL QUANTITIES

$P_{o1,2}$	Commanda signals to the controllable generators
$P_{N1,2}$	Command signals to the DC pole control
$P_{c1,2}$	Actual power transmitted signals

CHAPTER 1

INTRODUCTION TO THE HVDC POWER SYSTEM

1.1 An Historical Review of DC Transmission

Pratical application of the generation and transfer of electric energy began with the use of direct current, and the first power station in the world designed and built by Thomas E Edison in New York in 1882, supplied DC power from bipolar DC generators driven by steam engines. In spite of this, however, the advent and development of transformers, poliphase circuits and induction motors favoured the alternating current system of the generation, transmission and distribution of the electric energy (Kimbark, 1971).

The main reason for this is the ease with which the generated AC voltages can be transformed up to the AC voltages to be transmitted, and readily lowered again to the values required by the consumers. The fact that generation is inherently the production of alternating EMFs coupled with the advangs of AC transformation, is the basic reason for the widespread development of the AC system. Thus DC power played a secondary part for a long period in electricity history, and until 30 years ago was confined for use on industrial drives and traction.

The realization that over very long distances transmission of DC at high voltages might prove more economical than AC, has spurred the development of high voltage direct current (HVDC) technology.

In late 1954 the first commercial direct current transmission linked the island of Gotland to the mainland of Sweden and today several high-voltage direct current transmission

installations are in operation. These projects are listed in Table 1 which shows that the main applications for DC in order of importance are:

(a) underwater cable scheme
(b) long distance bulk transmission
(c) asynchronous tie or frequecy changer
(d) mixed overhead underground.

1.2 DC Application Considerations

The economic advantages of the use of DC lines accrue from less insulation, fewer conductors and smaller towers.

In addition, the technical advantages of a DC line over an AC line might sometimes justify its application.

The main technical advantages of DC lines are summarized as follows:

(a) greater power per conductor
(b) asynchronous operation
(c) ground return can be used
(d) rapid control of power flow

On the other hand the transfer of energy from one AC network to another by DC is only possible by transforming the energy of the AC network into a high-voltage DC energy (rectification) and by returning the DC to AC energy (inversion) at the other end of the DC line before connecting it into the receiving AC network. The solution of these problems has become possible after decades of development in the field of power conversion with the construction of mercury-arc valves at first stage and of thyristor valves in recent times (Uhlmann, 1975).

Scheme	Terminals	Year	Direct Voltage (kV)	Power (MW)	Length (km,mi) Overhead Line	Cable	Total	Remarks
Gotland	Västervik, Sweden	1954	100	20	0	96(60)	96(60)	Monopolar
	Visby, Gotland							Sea return
English Channel	Lydd, England	1961	±100	160	0	64(40)	64(40)	
	Echinghen, France							
Volgograd, Donbass	Volgograd, USSR	1962	100	90	474(294)	0	474(294)	
	Donetz Basin, USSR	1965	±400	720				
New Zealand	Benmore, Sout Id	1965	±250	600	570(354)	40(25)	610(379)	
	Hayward, North Id							
Konti-Skan	Göteborg, Sweden	1965	250	250	88(54)	87(54)	174(108)	Monopolar
	Alborg, Denmark							Sea return
Sardinia	Codrongianos Sardinia,	1966	200	200	290(180)	116(72)	406(252)	Via Corsica Homopolar
	San Dalmazio, Italy							
Vancouver	Arnott, British Columbia	1968	130	78	41(26)	32(20)	73(46)	First stage
	Vancouver Island	Ultimate	130	312				Final stage
Pacific NW-SW	The Dalles, Oregon	1970	400	1440	1372(853)	0	1372(853)	Three bridges
	Sylmar, California							per pole
Kingsnorth	Kingsnorth power plant		266	640	0	59(37)	59(37)	Each pole has a
	Beddington and Willesden (London)					82(51)	82(51)	different destination
Nelson River Manitoba	Radisson (Kettle Rapids)	Ultimate	450	3240	895(555)	0	895(555)	To be built in stages
	Dorsey (Winnipeg)							
Cahora-Bassa Mozambique	Songo, Mozambique Apollo, South-Africa	1979	533	1800	1414	0	1414	Built in 2 stages

TABLE 1

Moreover the conversion operations and the power transmission can only take place under the supervision of sophisticated control devices.

Thus converters and control apparatus considerably increase the costs of the DC transmission system.

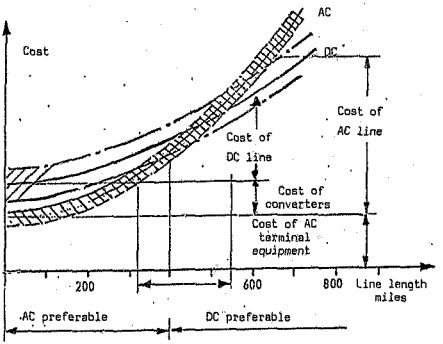


Fig. 1.1 Comparative costs of AC and DC transmission systems. Cigre report (1965 Cost).

A study carried out by the CIGRE working committee has evaluated the break-even line length which makes DC preferable to AC transmission (CIGRE REPORT, 1965).

1.3 Principles of DC Power Transfer

The transmission of energy from a generating network to the receiving one by DC requires two energy conversions (recti-

fication and inversion) at the ends of the DC line.

A schematic DC transmission system using two converter groups is shown in Fig. 1.2.

The DC power transmitted at the output of the rectifier is given by

$$P_t = V_t \cdot I_d \qquad 1.1$$

and the DC power received at the input of the inverter is given by

$$P_r = V_r \cdot I_d \qquad 1.2$$

Considering the transmission line loop resistance as R, the voltage drop in the line is $I_d.R$ and the power losses are $I_d^2.R$.

Transmitted current deduced from the above relationship is

$$I_d = \frac{V_t - V_r}{R} \qquad 1.3$$

ignoring the dynamic resistances given by the converters (see paragraph 3.1).

The direct voltage at the inverter side is maintained constant for any current value, which will vary with variations of the direct rectifier voltage. The DC transmission connection shown in Fig. 1.2 can therefore be represented by the equivalent circuit of Fig. 1.3, where the rectifier is replaced by a variable current generator and inverter by a constant voltage generator. Fig. 1.3 thus shows the schematic equivalent circuit of an HVDC system where the DC is transmitted at constant line voltage (see paragraph 3.1).

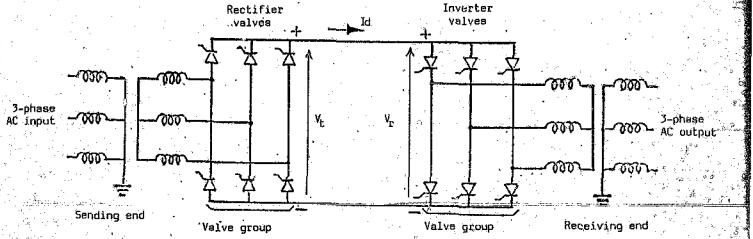


Fig. 1.2 Detailed HVDC link

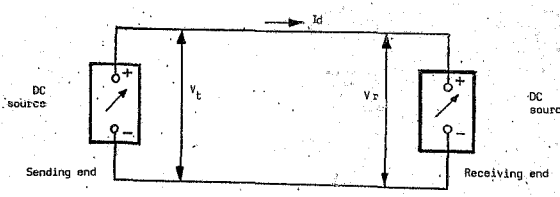


Figure 1.3 Simple DC link

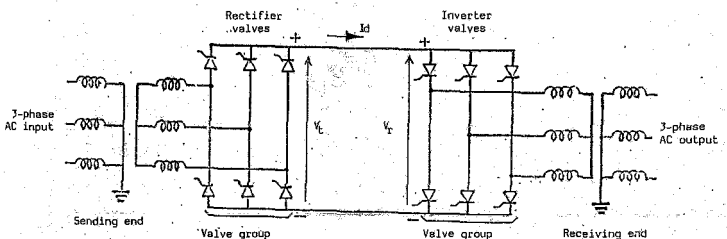


Fig. 1.2 Detailed HVDC link

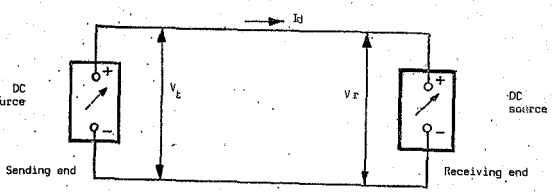


Figure 1.3 Simple DC link

Conversion is supervised by a converter control system, which is an essential part of any direct current transmission link. The main function of the control system is to regulate the power transmitted by the HVDC link to a predetermined pattern under steady state and transient conditions.

Moreover, in conjunction with fault detecting equipment, the control system takes action to clear certain faults, and to maintain the continuity of power flow in abnormal situations (Anderson et al, 1971).

1.4 The Cahora Bassa-Apollo Scheme

The Cahora Bassa-Apollo transmission connection was completed at the end of 1979 when the third and last project stage involving two new converter groups was finalized and put into operation. The realization of this project was possible when the final agreement was reached in 1965 following long negotiations between the Portuguese and South African governments. Both governments saw a mutual benefit which could be derived from the Zambezi water catchment in the gorge at Cahora Bassa "ideally suited for an arch dam", (Fig. 1.4).

Generation and export of energy at relative low cost and the agricultural development for the downstream indigenous populations was the philosophy on which the construction of the Cahora Bassa dam was based.

The contractual work for the construction and financing of the project was won by a consortium of 15 international companies (ZAMCO) from West Germany, France, Italy, Portugal and South-Africa.

Conversion is supervised by a converter control system, which is an essential part of any direct current transmission link. The main function of the control system is to regulate the power transmitted by the HVDC link to a predetermined pattern under steady state and transient conditions.

Moreover, in conjunction with fault detecting equipment, the control system takes action to clear certain faults, and to maintain the continuity of power flow in abnormal situations (Anderson et al, 1971).

1.4 The Cahora Bassa-Apollo Scheme

The Cahora Bassa-Apollo transmission connection was completed at the end of 1979 when the third and last project stage involving two new converter groups was finalized and put into operation. The realization of this project was possible when the final agreement was reached in 1965 following long negotiations between the Portuguese and South African governments. Both governments saw a mutual benefit which could be derived from the Zambezi water catchment in the gorge at Cahora Bassa "ideally suited for an arch dam", (Fig. 1.4).

Generation and export of energy at relative low cost and the agricultural development for the downstream indigenous populations was the philosophy on which the construction of the Cahora Bassa dam was based.

The contractual work for the construction and financing of the project was won by a consortium of 15 international companies (ZAMCO) from West Germany, France, Italy, Portugal and South-Africa.



Fig. 1.4 The gorge of Cahora Bassa

The ZAMCO consortium was subdivided into several sub-consortiums to fulfill the varius features of the civil and electrical engineering work.

The project entered commercial operation in three stages as follow:

(a) Stage 1 (26 March 1977)
It comprised the construction of the dam wall, underground power station, three turbo-generators, the converter stations of Songo (6 km away from Cahora Bassa dam) and Apollo (near Irene Pretoria, South Africa) and twin transmission lines 1 400 km long. On the completion of stage 1 the transmission of DC at limited operating voltages (266 KV) began, with the use of 4 converters (2 rectifiers and 2 inverters).

(b) Stage 2 (April 1978)
A fourt generator was added and two further converter groups were installed.

(c) Stage 3 (22 June 1979)
The two final converter groups were completed and the DC transmission was brought up to the rated capacity of 1 920 MW (Olivier, 1977).

1.5 Cahora Bassa Generating Plant

The station is equipped with 5 generating units consisting of:

(a) 5 vertical Francis type turbines giving a nominal output of 415 MW at a nominal speed of 107,1 rpm, and water consumption of 452 m^3/second.

(b) 5 generators each of 480 MVA at the nominal rotation given by the Francis turbines. They have static excitation through thyristors, a rotor diameter 13 m and a weight of 960 tons.

(c) 5 penstocks, 2 tailrace tunnels, 2 surge vessels and the 220 KV feeders to the bus-bars of the rectifier station (Songo) 6 km away are other relevant installations of the generating plant of Cahora Bassa scheme.

1.6 Songo-Apollo DC Transmission

The AC energy generated at Cahora Bassa power station is conveyed to the bus-bars of Songo sub-station 6 km away, where it is converted by the rectifier bridges into DC energy and transmitted to the inverter sub-station of Apollo via twin overhead lines 1 km apart and 1 400 km long. At the inverter the DC energy is converted into AC before being injected into Escom network.

On completion, the Songo-Apollo DC transmission scheme was:

(a) the highest voltage (± 533 KV) DC transmission system in the world, nearly 100 KV higher than the ± 450 KV Nelson River scheme

(b) the largest in power transmission capacity (1 920 MW)

(c) the longest transmission circuit (1 400 km)

(d) the first power transmission scheme to be entirely dependent on thyristor valves and the first to mount such valves out of doors

(e) the first scheme to use four valve bridges in series on each side of the earth

(f) the first scheme not provided with by-pass valves, but using short-circuiting switches (overcurrent diverters) for valve protection in certain extreme conditions.

The different modes of DC power transmission used in the Songo-Apollo scheme are described in paragraph 2.1.

1.7 Thyristor Valves Used at the Songo and Apollo Converter Stations

A very important innovation in this DC scheme is the use for the first time of high voltage thyristors assembled in modules to form the bridge valves. They were designed and manufactured by a ZAMCO study group TSE (Siemens, AEG Telefunken and Brown Boveri), * who collaborated in a research project at Mannheim Rheinau (Germany).

* Note: This type of thyristor, tried in low voltage application is designated in the catalogues as type B.St.P.05.110.

Thyristors are serially mounted in a stack, numbering 7 (stage 1) or 6 (stages 2 and 3). Each thyristor is electrically paralleled with its partner in the adjacent stack.

There are four stacks in a tier (24 or 28 thyristors) and 10 tiers form a valve. The number of thyristors to be connected in series to form a valve was based on the concept that the valve has to withstand a surge voltage of 3,05 times the rated direct voltage. The factor 3,05 determines the valve withstand voltage which is 10% above the maximum calculated surge diverter spark-over, plus a further 20% to allow for thyristor redundancy and unequal voltage distribution.

A valve unit comprises two valves mounted in a common steel tank with two high voltage bushings, the one forming the positive terminal and the other the negative terminal. The tank itself is connected to the point where the two valves are joined together and hence is at the voltage with respect to ground of the transformer phase connection. (see Fig. 1.5)

The thyristors are forced oil-cooled and the whole valve is insulated under oil. The voltage protection for the valves is provided by means of surge diverters, which limit the voltage to the required values for surge wave-front bigger than 1 μs. Each valve is moreover protected against surges having a shorter wave-front time than 1 μs by a saturable reactor.

Ancillary valve circuitry is also provided in order to:

(a) Control the thyristor voltage grading

(b) Reduce dynamic stresses on the thyristors

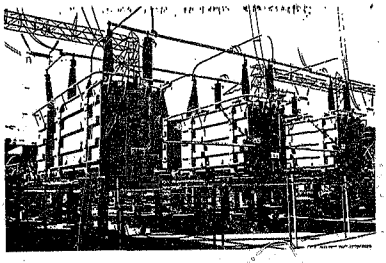


Fig. 1.5 Valve tanks forming a bridge
(Apollo inverter station)

(c) limit the surge amplitude of the reverse voltage at the end of the conducting period. (see Fig. 1.6)

The firing pulse for each thyristor gate is derived from a common pulse transformer (firing pulse loop), which forms the central core of each valve (Lane and Calverley, 1970b).

1.8 *Outline of the Dissertation*

The paragraphs of chapter 2 provide a brief analysis and representation of the circuits and main functions which have a predominant effect on the performance of HVDC transmission. This preliminary description appears necessary and helpful for easy understanding of the operations carried out by the automatic control system in an HVDC scheme, which will be expounded, under its different features in Chapter 3,4 and 5.

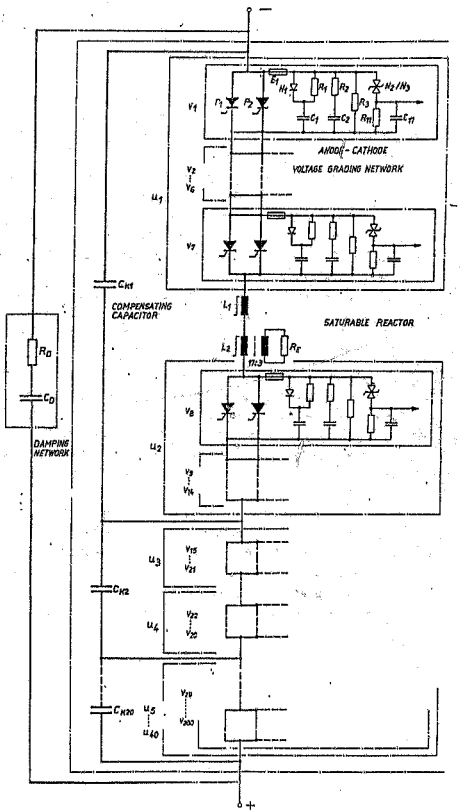


Fig. 1.6 Thyristor stacks forming a valve, valve damping network and voltage grading network at Apollo (Zamco TSE, 1971).

Chapter 3 outlines the essential objective of the automatic control which is to ensure stable power transmission during both steady state and unfavourable conditions. In other words the operations performed by the control at the rectifier end, are correlated with those carried out at the inverter end, and the purposes of such operations are explained. Also in Chapter 3, the main circuit of the control at the rectifier as well as at the inverter side are discussed mainly in respect of characteristics they have to posses to cope with the different problems related to DC power transmission. Problems arising on the rejection of DC power are also briefly discussed.

Chapter 4 is occupied entirely by the analysis of the control system which operates at any inverter bridge, to keep the inverter output direct voltage constant. Some disturbances which may effect the inverter bridge control and the requirements for limitation of such effects on the bridge control are discussed.

Finally in Chapter 5, the automatic control operating at Songo-Apollo scheme is analysed, taking into consideration two important means of protection. The way the control reacts on the occurrence of commutation failure at the inverter side is described and the way it protects the line on the occurrence of line earth fault without compromising total DC transmission.

References

1. Anderson, D.M. et al. (1971) An introduction to HVDC, Paper for Westinghouse Canada limited, Hamilton, pp. 2-55.

2. Cigre report (1965) Costs of AC and DC transmission lines, Paris, 1965.

3. Kimbark, E.W. (1971) Direct current transmission, 1st ed. New York: Wiley, 1972, pp.1.

4. Lane, F.J.; Calverley T.E. (1970) Proposal for application of AEG/SIEMENS/BBS tyristors valve technique, document submitted for Cahora-Bassa - Apollo HVDC project, Brighton, October 1970, pp. 1-28.

5. Olivier, H. (1977) Great Dams in Southern Africa, 1st ed. Cape Town: Purnell, 1977, pp. 75-82.

6. Uhlmann, E. (1975) Power transmission by direct current, 1st ed. Heidelberg, New York: Spring-Verlag, 1975, pp. 1.

7. Fig. 1.6 Zamco, TSE. (1971) Valve and associated equipment, Report SS40.414 for the final design of Cahora Bassa-Apollo scheme, fig. no. 551/TSE-C40-002. pp. 7.

CHAPTER 2

BASIC THEORY OF HIGH VOLTAGE DC TRANSMISSION SYSTEMS

2.1 Operating Modes of a DC Transmission System

There are four possible modes for transmitting DC power from the rectifier to the inverter. These are:

(i) the bipolar mode, Fig. 2.1a (the normal mode of transmission at Songo-Apollo scheme)

(ii) the monopolar mode, Fig. 2.1b (used under line fault conditions)

(iii) the parallel mode, Fig. 2.1c (used under emergency conditions)

(iv) the homopolar mode, Fig. 2.1d (not used on the Songo-Apollo scheme) (Kimbark, 1971a).

2.2 Three-phase Converters

Converters are devices that convert AC to DC and DC to AC. (fig. 2.2a). At the sending terminal (at Songo) the converters are called rectifiers (AC to DC), and at the receiving terminal (at Apollo), they are called inverters (DC to AC). The converters used in the Songo-Apollo scheme use the standard Graetz bridge configuration using thyristors (SCRs) instead of diodes. In the older schemes, mercury-arc valves were used instead of SCRs. The transformer of a converter bridge can be of star-star or delta-star configuration.

A terminal consists of groups of an equal number of converters in series on the DC side. The neutral point between the two groups of converters is grounded through earth electrodes at

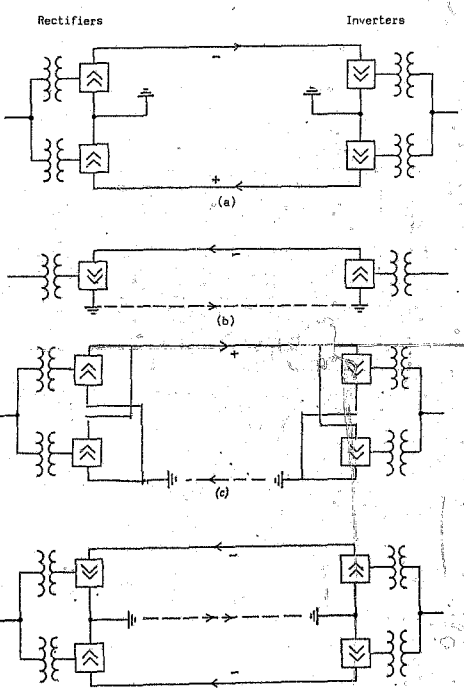


Fig. 2.1 DC transmission operating modes
a) bipolar; b) monopolar
c) parallel; d) homopolar.

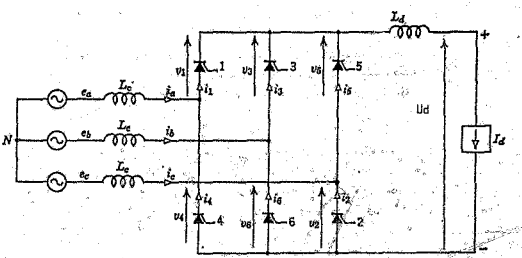


Fig. 2.2a Bridge converter - schematic circuit for analysis. The valves are numbered in their firing order.

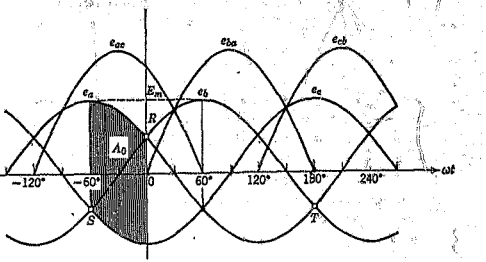


Fig. 2.2b Waves of instantaneous EMFs of AC source: line to neutral, e_a, e_b, e_c; line to line, e_{ac}, e_{ba}, e_{cb}. (Kimbark, 1971).

each end. In the event of a fault on one conductor, the other operates with half the rated load (monopolar mode, Fig. 2.1b).

2.3 Rectification and Inversion in DC Transmission

In the bridges shown in Fig. 2.2a used for conversion of AC or DC power, the thyristors or valves used in the Graetz configuration have to be fired when the line-to-line voltage across them is positive.

The line-to-line voltages are given at the secondary winding of bridge transformers by 6 possible combinations of the transformer secondary to neutral voltages ($e_{ab}=e_a-e_b=-e_{ba}$, $e_{ac}=e_a-e_c$, $e_{bc}=e_b-e_c$, $e_{ba}=e_b-e_a$, $e_{ca}=e_c-e_a$, $e_{cb}=e_c-e_b$) as can be seen in Fig. 2.2b.

From the theory of the rectification process of the Graetz bridge using no controlled rectifying elements (diodes Fig. 2.3) , the direct output voltage on load condition is given by the upper envelope of the line-to-line voltage (Fig. 2.4b). The average of such envelope is

$$Udo = 3\sqrt{3}\,(Em/\pi) \qquad 2.3.1$$

where Em is the amplitude of the secondary to neutral voltage. It is important to emphasize that due to the relationships of the secondary to neutral voltages, only two diodes in series are conducting and both of them for one-third cycle (120°). For example, diode 1 carries the load current with diode 2 until diode 3 commutates and takes over to carry the load current together with diode 2, and so on. Commutations are consequently occuring spontaneously every one-sixth cycle (60°) indicated in number order according to Fig. 2.3.

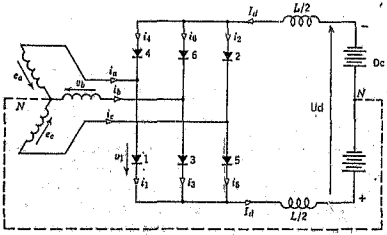


Fig. 2.3 Standard Graetz rectifier.

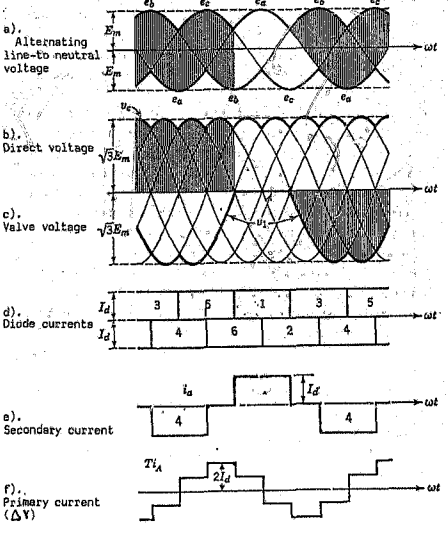


Fig. 2.4 Graetz rectifier waveforms.
(Kimbark, 1971).

Fig. 2.4e gives the waveshape of the current flowing in the secondary winding of the bridge transformer due to the cycling commutation of the diodes.

The use of thyristors on the Graetz bridge makes the spontaneous commutations and the flowing of the load current impossible unless the thyristors are appropriately fired on their gate. The firing must be provided to cause commutation every 60° and under conditions of positive voltage across the valve. By using thyristors it is possible to delay the firing angle theoretically from 0° to 180° (see Fig. 2.2b).

Variations of the firing angle within such range give a direct voltage varying as shown in Fig. 2.5.

Up to 90° the direct voltage presents a positive polarity and the load current is flowing in the direction permitted by the thyristors in agreement with the voltage polarity. Thus, there is a direct power flow which is the result of the rectification. When the delay firing angle exceeds 90°, the direct output voltage changes to the negative polarity and opposes the load current flow. A reverse power flow takes place and the power inversion is obtained by feeding the AC system with the reverse power. From the point of view of power transmission, the rectifier conversion is followed by a transmission of DC power by transmission of DC current and generation of DC voltage by the inverter on receiving the transmitted current.

It is possible to derive from the last statement that the DC transmission takes place between two systems, which behave as current (rectifier) and voltage (inverter) generators respectively. Because the inverter is the receiving end of the DC transmission the inverter DC voltage has to be maintained lower

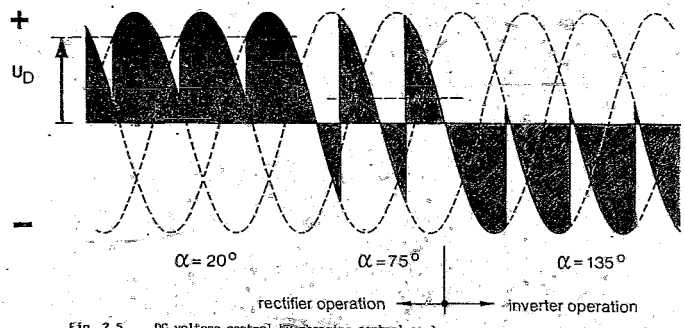


Fig. 2.5 DC voltage control by changing control angle.

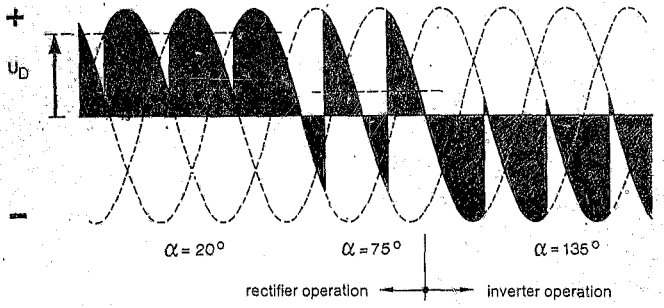


Fig. 2.5 DC voltage control by changing control angle.

than the rectifier DC voltage in order to permit the current flow (Calverley, 1954a).

2.4 Definition of the Firing Angles α and β, Overlap Angles μ_α, μ_γ and Extinction Angles δ and γ

The positive crossing voltage of 0° and the negative crossing voltage of 180° have been conventionally agreed as the angle references for the rectifier and the inverter firing angle respectively.

Rectification is characterized by the firing angle α (alfa) which is delayed in respect of the angle reference (0°) while the firing angle β (beta) advanced in respect of the angle reference 180° indicates inverter operation. (See *Fig. 2.6a, 6b*).

The two firing angles are related by:

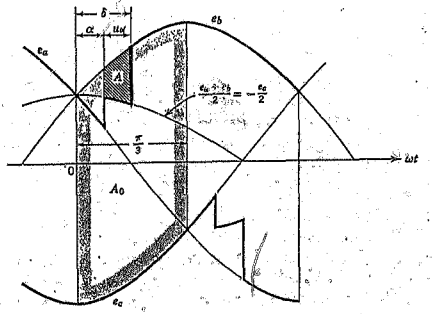
$$\alpha = 180° - \beta \qquad 2.4.1$$

and both can be used to represent the rectification and the inversion.

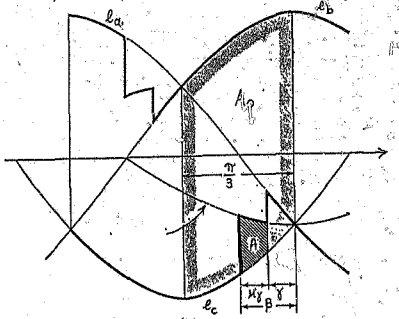
In the rectifier operation, the valve commutation takes place at the angle $\delta = \alpha + \mu_\alpha$. (delta)

δ is defined as the extinction delay angle for rectification. μ_α is the overlap angle which is dependent on the AC reactance affecting the rate of current change during commutation. In the inverter operation the extinction angle is named γ (gamma) and is related to the advanced firing angle β by $\beta = \gamma + \mu_\gamma$. (Fig. 2.6b) where μ_γ is the inverter overlap angle.

The two overlap angles μ_α and μ_γ are increasing on the



(a)



(b)

Fig. 2.6 (a) Rectification angles;
(b) Inversion angles.

decreasing of α and γ respectively, and also dependent upon the increasing of μo defined as the overlap angle for $\alpha = 0$ or $\gamma = 0$. μo decreases with the increase of the converter internal voltage Udi* according to the relation:

$$\cos \mu o = 1 - 2 \cdot \left[\frac{2 (Dxt + Dxv)}{Udi} \right] \qquad 2.4$$

where Dxt and Dxv represent the transformer reactance and valve reactance voltage drops respectively. A rapid calculation of μ_α and μ_γ can be obtained by plotting (Fig. 2.7) the relationship between α, μo and μ_α (γ, μo, μ_γ) for different direct currents. The relationship between the above functions are given by:

$$\cos (\alpha + \mu_\alpha) = \cos\alpha + \cos \mu o - 1 \text{ (rectification)} \qquad 2.4.4$$

$$\cos (\gamma + \mu_\gamma) = \cos\gamma + \cos \mu o - 1 \text{ (inversion)} \qquad 2.4.5$$

At small γ extinction angles the overlap angle μ_γ assumes very high values for any DC current. That may adversely affect the thyristor commutation and a safety combination of μ_γ and γ values must therefore be chosen for any DC current (commutation limit line Fig. 2.7) and a very small advance β angle. (Generally the smallest γ, which has a sufficient safety margin from the recovery-angle of the thyristors is chosen first and then from the plotted curves of Fig. 2.7 μ_γ can be derived). The relationship between γ and thyristor recovery-angle is given in Chapter 5, paragraph 1.4.

2.5 No-load Voltage and the Output Direct Voltage at the Converters

The no-load voltage of a converter has been expressed by $Udi = \frac{3\sqrt{2}}{\pi} E_1 = 1,35 E_1$ **. It depends on the position of the transformer tap-changer because the transformer ratio given for proper AC line-to-line input voltage to the converter

NOTE * Converter internal voltage is also defined as no-load voltage of the conversion (see paragraph 2.5)

NOTE ** E_1 is the amplitude of the line-to-line voltage.

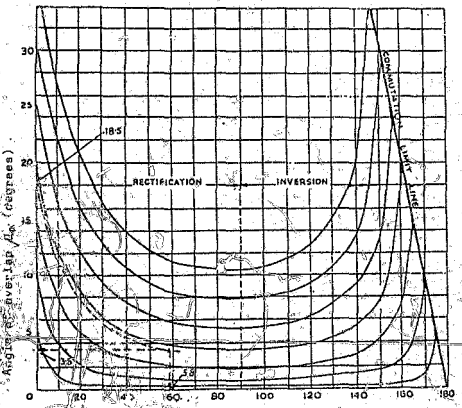


Fig. 2.7. Curves of μ_α (μ y) plotted from equation 2.4.4 and 2.4.5 (Calvery, 1954).

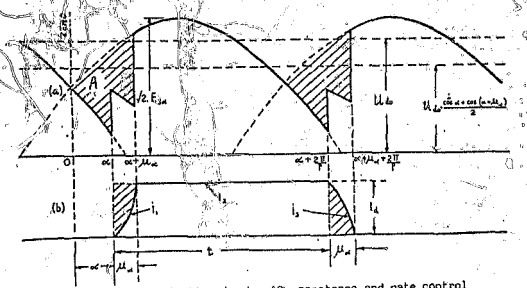


Fig. 2.8. Modification due to AC reactance and gate control of: a) DC voltage wave-form; b) secondary current.

is determined only by the tap-changer tapping. The no-load converter voltage can be obtained by the simple calculation of the equation

$$Udi = 1{,}35\ E_1 \qquad 2.5.1$$

when the AC primary voltage and the position of the tap-changer are known.

The converter direct output voltage can be derived from the no-load converter voltage by taking into consideration all the causes of voltage drops which are affecting the final value of the converter output voltage.

In both converter terminals, voltage drops are caused by valve resistance, firing angle α for rectifier and γ extinction angle for the inverter, valve reactance, transformer resistance and finally transformer reactance. The output direct converter voltage can thus generally be expressed by

$$Ud = Udi - \Sigma(\text{converter voltage drops}) \qquad 2.5.2$$

(For the inverter it must be emphasised that the valve resistance and the transformer reactance drops are quantities to be added to Udi because of the reverse power flow).

2.6 Direct Voltage Drops due to α and $U\alpha$

The rectifier output direct voltage drop due to the firing delay angle α is indicated in Fig. 2.8a as area A. From the same figure it can also be clearly seen that the drop in direct voltage $Ud\alpha$ * is increased by the presence of the overlap angle $\mu\alpha$. By integration, A is expressed by:

* NOTE $Ud_\alpha = Udi - Udi \cdot \cos\alpha$

$$[Udi\ (1-\cos\alpha\ ) + Udi/2].\ (\cos\alpha - \cos\delta\ ) = A = Ud \qquad 2.6.1$$

where the first term is the voltage drop due to the delay angle α and the second term is the drop as the result of the overlap angle μ *. From equation 2.6.1 and the general expression of the rectifier output direct voltage, described in paragraph 2.5, a new expression for the rectifier direct voltage is derived

$$Ud = Udi.\frac{(\cos\alpha + \cos\delta)}{2}$$

which, as an approximation, can be re-written:

$$Ud = Udi.\cos\alpha \qquad 2.6.2$$

The last expression show the dependence of the rectifier direct voltage on the firing delay α angle.

The inverter output direct voltage can be similarly expressed by

$$Ud = Udi.\cos\gamma \qquad 2.6.3$$

The DC converter direct voltage variation as a function of α is represented in Fig. 2.5 where the parameter α is used to vary the DC voltage in the rectifier as well in the inverter angle dominion of conversion (Kimbark, 1971b).

2.7 The Secondary Current Wave Forms and the Power Flow through a Converter

The transformer inductance permits the secondary currents (i_a, i_b, i_c) to vary at a finite rate when a valve commutates from off to on state and viceversa. Referring to Fig. 2.9

* Since $\delta = \alpha + \mu_\alpha$

for instance, the secondary current i_b of a rectifier starts to flow at the instant that valve 3 starts to conduct having been ignited with a delay angle α respect to the line to line voltage e_{ba}. At the same instant valve 1 starts to commutate towards its off state and consequently the secondary current i_a also decreases at a finite rate. Therefore if we consider the equivalent circuit of the rectifier bridge (Fig. 2.9) during commutation from 1 to 3 the balance of inductive potentials and the line to neutral voltages e_b and e_a is given by

$$e_b - e_a = Lc\, di_3 / dt - Lc\, di_1 / dt \qquad 2.7.1$$

Since $e_b - e_a = e_{ba}$ (paragraph 2.3) and $i_3 = i_b$ and moreover $e_{ba} = \sqrt{3}Em \sin\omega t$ from the theory of a three phase transformer, the expression (2.7.1) can be re-written as:

$$\sqrt{3}Em \sin\omega t = Lc\,(di_b/dt - di_a/dt) = 2Lc\, di_b / dt \qquad 2.7.2$$

because during the commutation current, voltage balance in the same circuit of Fig. 2.9 is given by

$$di_a / dt = - di_b / dt \qquad 2.7.3$$

By definite integration from α to angle ωt of the expression 2.7.2, it is possible to obtain the secondary current waveform i_b as

$$i_b = (\sqrt{3}Em / 2\omega Lc)(\cos\alpha - \cos\omega t) \qquad 2.7.4$$

meanwhile during commutation the expression of i_a will be

$$i_a = Id - i_b = Id - (\sqrt{3}Em / 2Lc)(\cos\alpha - \cos\omega t) \qquad 2.7.5$$

In conclusion it can be said that each of the secondary currents

i_a, i_b, i_c is composed of three components I_1, I_2, I_3 (see Fig. 2.8b). I_1 and I_3 are given by equation (2.7.4) and (2.7.5) respectively and I_2 is equal to the load current Id. The Fourier analysis gives a fundamental component of the secondary current (i_a, i_b, i_c) equal to:

$$I_{ilo} = Id \cdot (\sqrt{2}/\pi) \cdot \sin \pi/p \qquad 2.7.6$$

(ignoring the influence of μ_α).

The power flow through the rectifier equipment will be thus:

$$P = Id.(\sqrt{2}/\pi).\sin \pi/p.\left[Udi.\cos\alpha + \cos(\alpha + \mu_\alpha)\right]/2 \qquad 2.7.7$$

From the last expression we can derive the current fundamental secondary current:

$$I_{ilo} = Id \cdot (\sqrt{2}/\pi) \cdot \sin \pi/p \cdot \left[\cos\alpha + \cos(\alpha + \mu_\alpha)\right]/2 \qquad 2.7.8$$

The power component correction factor is defined as:

$$\omega(l\alpha)p = \left[\cos\alpha + \cos(\alpha + \mu_\alpha)\right]/2 \qquad 2.7.9$$

It can be also demonstrated that the reactive power component factor is given by:

$$\omega(l\alpha)r = \frac{2\mu_\alpha + \sin 2\alpha - \sin 2(\alpha + \mu_\alpha)}{4\left[\cos\alpha - \cos(\alpha + \mu_\alpha)\right]} \qquad 2.7.10$$

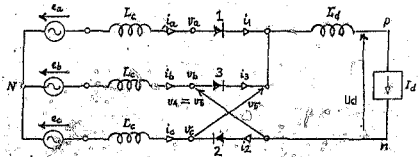


Fig. 2.9 Equivalent circuit of a converter during commutation

The variations of both factors as functions of α and $\mu\alpha$ are shown in Fig. 2.10. In the same figure (2.10) the phase γlsa of the fundamental secondary current is also shown.

It can be demonstrated that cos (γlsa) represents the power factor for a DC transmission (Calverley, 1954b).

In conclusion, the direct rectifier power flow takes place for values of α between 0° and 90°. The reactive power reaches the maximum at α = 90° and decreases again for α values increasing towards 180°, but active power is now flowing in reverse mode (inversion).

The relation between the delay angle α and the phase displacement shown in Fig. 2.11 confirms the conclusion reached by examination of the curves describing the power transmission through a converter.

All functions characterising the rectifier and inverter operations are shown in Fig. 2.12 and 2.13 respectively. A very significant feature used to distinguish between rectifi-

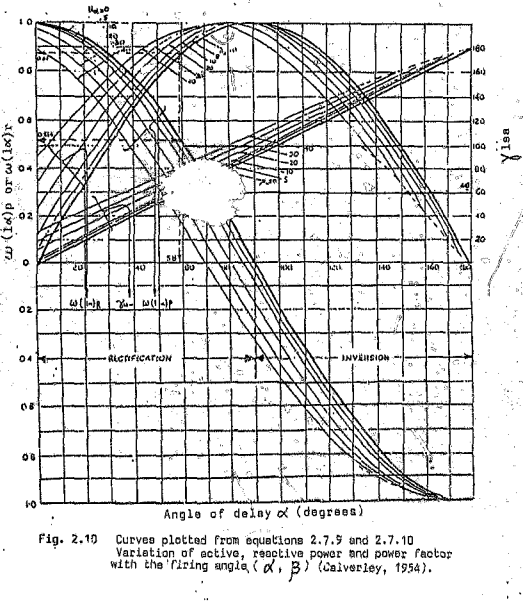


Fig. 2.10 Curves plotted from equations 2.7.9 and 2.7.10 Variation of active, reactive power and power factor with the firing angle (α, β) (Calverley, 1954).

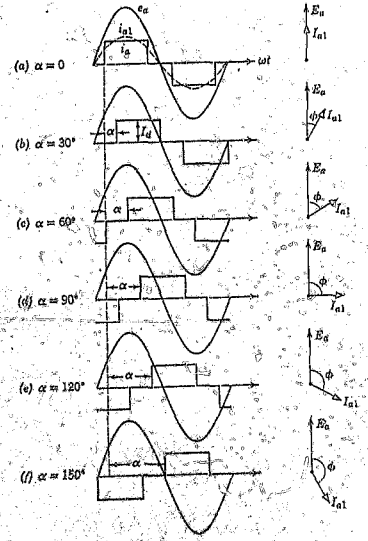


Fig. 2.11 Relation between ignition delay and phase displacement. (Kimbark, 1971).

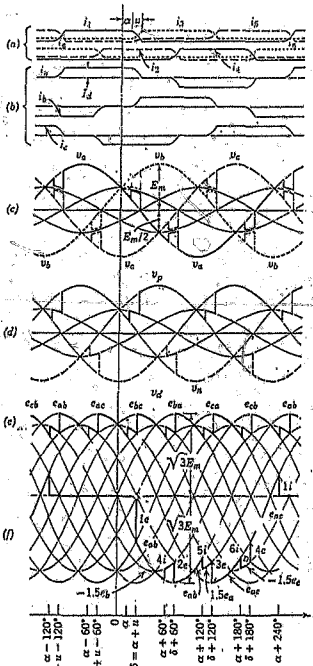


Fig. 2.12 Instantaneous currents and voltages of three-phase bridge converter with $\lambda = 15°$ and $\mu_\alpha = 15°$. (Kimbark, 1971).

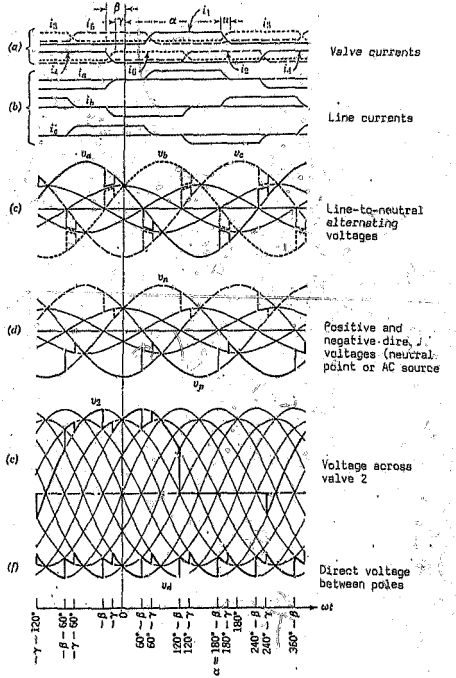


Fig. 2.13 Wave forms of currents and voltages of three-phase bridge inverter $\alpha = 150°$, $\beta = 30°$.

cation and inversion is the wave form of the voltage across the valves of a bridge working as inverter (Fig. 2.14a).

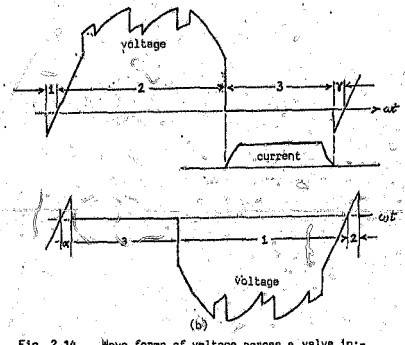


Fig. 2.14 Wave forms of voltage across a valve in:- a). inverter and b). rectifier: 1. inverse period; 2. blocking period; 3. conducting period.

and rectifier (Fig. 2.14b) respectively).

2.8 SUMMARY

This chapter has reviewed the operating modes of high voltage DC transmission systems and the basic theory of operation of three-phase converters. The accepted methods of calculating the steady state performance of an HVDC transmission scheme have been briefly discussed as well as the principles of DC power flow and the relationships between the main functions

regulating power transmission. The relationships used by the project group to carry out the basic calculations of the rectifier and inverter parameters are based on the following inter-related design data:

(a) Direct current Id.
(b) Output DC voltage UD.
(c) Control angles α, β
(d) Rectifier EMF Udi.
(e) AC system voltage.

For a good understanding of the following chapters, definitions of the controlled and uncontrolled angles which originate during the valve firing were given. In conclusion, a comparative correlation between the rectifier and inverter operational functions has been explained.

References

1. Calverley T.E. (1954a) The flow of power and reactive components in rectifier and inverter equipment, English Electric Journal, vol. xiii, no. 5 and 6 pp. 21-23.

2. Fig. 2.7 Calverley T.E. The flow of power and reactive components in rectifier and inverter equipment, English Electric Journal, vol. xiii, no 5 and 6, pp. 21.

3. Calverley T.E. (1954b) The flow of power and reactive components in rectifier and inverter equipment, English Electric Journal, vol. xiii, no. 5 and 6, pp. 19-20.

4. Fig. 2.10 Calverley T.E. The flow of power and reactive components in rectifier and inverter equipment, English Electric Journal, vol. xiii, no. 5 and 6, pp. 22.

5. Kimbark E.W. (1971a) Direct Current transmission, 1st ed. New York: Wiley, 1971, vol, pp.11-12.

6. Fig. 2.2.b Kimbark E.W. (1971) Direct current transmission, 1st ed. New York: Wiley, 1971, vol. 1, pp. 73.

7. Fig. 2.4 Kimbark E.W. (1971) Direct current transmission, 1st ed. New York: Wiley 1971, vol. 1, pp. 59-60.

8. Kimbark E.W. (1971b) Direct current transmission, 1st ed. New York: Wiley, 1971, vol. 1, pp. 80-88.

9. Fig. 2.11 Kimbark E.W. (1971) Direct current transmission, 1st ed. New York: Wiley, 1971, vol. 1, pp. 78

10. Fig. 2.12 Kimbark E.W. (1971) Direct current transmission, 1st ed. New York: Wiley, 1971, vol. 1, pp. 109.

CHAPTER 3

CONTROL ASPECTS OF HVDC SYSTEMS

This chapter deals with the main features of the automatic control operating at Songo - Apollo converter system in relation to the fundamental principles of HVDC transmission. The physical structure of the most important circuits designed to perform control operations in the converters, are described. Their functions on determining system behaviour in different working situations (steady-state condition, transients and the occurrence of certain failures and faults) are explained with the aid of figures, oscillograms and specimen design calculations furnished by the planning and testing teams before and during the commissioning of the Cahora Bassa - Apollo scheme.

In addition, based on our direct experience, the causes of disturbances and their effects on the performance of the control system, are studied in connection with some of the most significant circuit arrangements at Apollo inverter station. (see Chapter 4).

3.1 Control Requirements of an HVDC System

In the development of the automatic control systems for HVDC conversion, the philosophy adopted is based generally on the following concepts:

3.1.1 Maintaining the system current at a steady-state value through the combined rectifier and inverter regulating processes, and limiting the maximum current to protect the current - carrying devices.

3.1.2 Varying the firing angle of the bridge valves to provide a fast, dynamic response to system changes.

This also means that the fluctuation of current due to the alternating voltage fluctuation must be limited by the automatic control.

3.1.3 Accurately timing the firing pulses for steady state operation.

3.1.4 Having the ability to operate with weak and unstable AC system.

3.1.5 Maintaining the power factor as high as possible so that

- the maximum power rating for each converter is obtained
- dangerous stresses on valves and damping circuits are reduced
- voltage drops at the AC terminals of the converters due to load increases, are limited.

3.1.6 Computation of the optimum power to be transmitted for given DC current and voltage ratings as by power demand.

In addition to meeting these basic requirements, converter automatic controls have to cope with many other needs, such as the transient periods of line energization, the switching on and off of the bridges and the occurrence of abnormal events and failures (Reeve et al., 1972).

3.2 Current and Voltage Control in HVDC Transmission

In dealing with general matters concerning rectification and inversion on HVDC transmission schemes, it is standard

practice to represent converters as two separate units: the current generator (rectifier) and the voltage generator (inverter), connected by a common current transmission line. (Fig. 3.1).

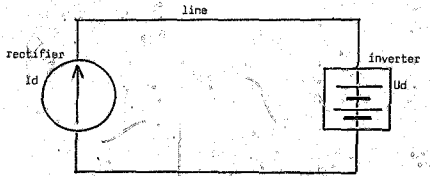


Fig. 3.1 Schematic DC link representation

Whe dealing with automatic control, however, this method of representntion is insufficient as it does not illustate the fundamental concept upon which a HVDC system is based.

The modes of transmission in a HVDC system are constant voltage with adjustable current, or constant current with adjustable voltage, where the adjustment is made under closed control loop. The modes of transmission are represented schematically in Fig. 3.2. One block, "A", represents all the distributed control operations performed at the rectifier and at the inverter, with objective of maintaining the rated power transmission constant. From the same schematic, it is clear that the automatic control system has a current and voltage reference from which it performs its control action for obtaining maximum power transfer within defined stability limits, and with guaranteed protection.

The theoretical converter control illustrated in Fig. 3.2, becomes a practical reality in the Songo - Apollo scheme, as shown in the Fig. 3.3 block diagram. The diagram shows the system symmetrically disposed in both stations. If we

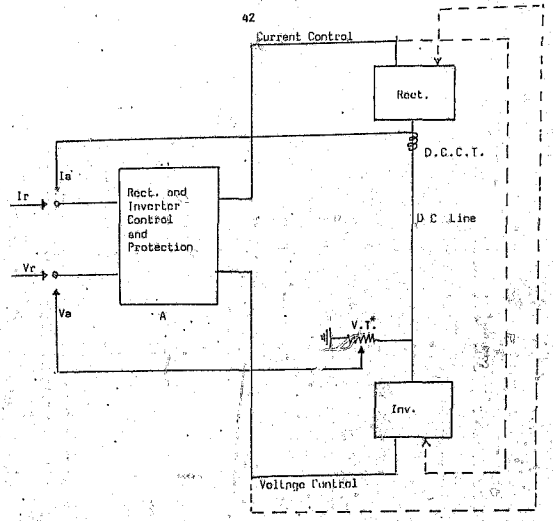


Fig. 3.2 General automatic control block diagram of a DC transmission system.

consider the converter system in the steady-state working condition, the transmission of current along the DC line is assured by the rectifier Id controller and by the inverter γ extinction angle controllers. The Songo - Apollo HVDC link** can be considered a constant voltage system, which means that changes in power transmission are only obtained by current changes. A DC power transmission system however is normally operated at its maximum permitted

* Voltage Divider
** HVDC link means HVDC transmission system

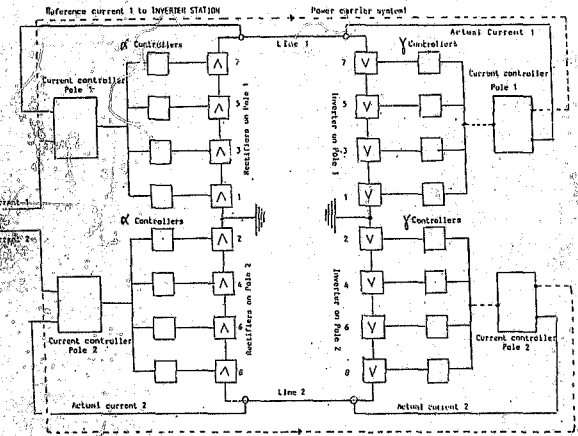


Fig. 3.3 Basic automatic control for DC transmission.
(Songo - Apollo scheme).

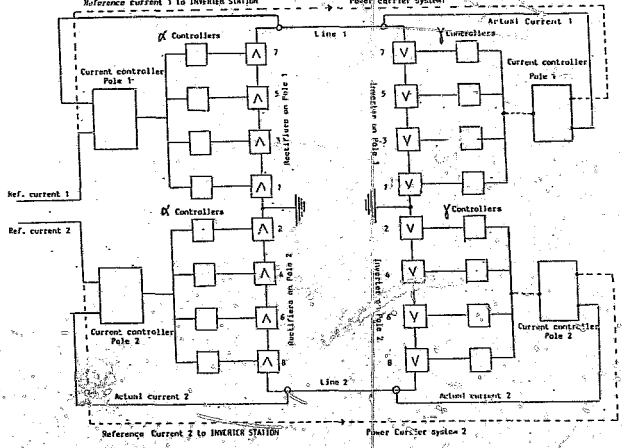


Fig. 3.3 Basic automatic control for DC transmission. (Sango – Apollo scheme).

load (maximum current) and the only possible way to very the power transmitted by a certain amount in the steady state condition is by changing the line voltage with the converter transformer tap-changer. Therefore an HVDC power transmission system at its maximum load also behaves as a constant current system and as such is protected against overload transients. From these considerations we conclude that the rectifier current regulator permits a rapid energization of the DC line (from zero to the maximum power) with restrained line conductor power losses, and at the same time prevents the growth of dangerous current peaks by fixing a maximum current limit (Kimberk, 1971a).

The table in Fig. 3.4 gives the values of line voltage, current and power measured at the Apollo inverter station when only one converter group is in operation (monopolar mode) and also in case of 6 converter groups in operation (bipolar mode). The figures on the table indicate that the DC line energization is actuated by the gradual increasing of the current, which leads to a DC power increase. The increase of DC transmitted power ends when the current reaches the maximum permissible limit (full load 1 800 A).

The rectifier current regulator controls the current by changing the delay firing angle α (see Chapter 2) and consequently the output rectifier voltage which is proportional to the function $\cos\alpha$. The proportional factor is the rectifier internal no-load voltage (see Chapter 2), regulated by the transformer tap-changers. In steady state (full load) power transmission, the delay angle α assumes a value of between 19° and 13° for a fixed position of transformer tap-changers.

The tap-changers are de[illegible] rease the rectifier voltage in case of $\alpha > 1$[illegible] increase the rectifier

Power from Songo	Bipolar operation 4 + 4 Converter Groups		Monopolar operation 1 + 0 Converter Groups		Power at Apollo
MW (AC)	KV(DC)	KA(DC)	KV(DC)	KA(DC)	MW (AC)
50			126.4	0,38	39
100				1,00	78
150				1,13	115
200				1,50	144
240			117	1,80	164
250					
300					
350					
400/1*					
440					
450					
480					
500					
550					
600					
650	492**	0.61			619
700		0,66			666
720		0,68			684
750		0,70			712
800/2*		0,75			758
850		0,80			804
880		0,83			831
900		0,84			850
950		0,89			895
960		0,90			901
1000		0,94			911
1050		0,98			985
1100		1,03			1031
1150		1,08			1075
1200/3*		1,13			1120
1250		1,17			1164
1300	479	1,22			1209
1320		1,24			1226
1350		1,27			1252
1400		1,31			1297
1440		1,35			1331
1450		1,36			1340
1500		1,41			1383
1550		1,45			1427
1600/4*	474	1,50			1469
1650		1,5			1512
1680		1,39			1538
1700		1,59			1555
1750		1,64			1568
1760		1,65			1606
1800		1,69			1610
1850		1,73			1682
1900		1,78			1723
1920/5*	468	1,80			1741

Fig. 3.4 Assumptions:
(a) Line resistance = 19Ω
(b) Aux. losses Songo & Apollo = 8 MW
(c) Songo bridge DC volts = 133,3 kV

* Maximum power of 1, 2, 3, 4, or 5 Generators
** One Pole DC Voltage

voltage in case of $\alpha < 13°$, so that α will be held between 13° and 19° during steady working conditions. Moreover, the table of Fig. 3.4 indicates that the line voltage measured at the Apollo inverter decreases slightly as the current is increasing. This is due to the rectifier output voltage dropping when current increases. Since the relationship between the line current and voltages at the DC terminals in the steady-state is given by the Ohm's law

$$Id = \frac{Ud1 - Ud2}{R_L + R_{c1} - R_{c2}}$$

(where Ud1 and Ud2 are the internal voltages of rectifier and inverter respectively; R_L the line resistance, Rc1 and Rc2 the commutating rectifier and inverter resistance respectively), to obtain a current as linear function of Ud1 - Ud2, the rectifier voltage drop for [illegible]nt increase has to be compensated by a correspond[illegible]fter voltage drop.

The transmitted line current is evaluated by the inverter tap-changer control system which operates to correct the inverter voltage so as to ensure the aforementioned system current - voltage linearity. The inverter voltage decrease [illegible]strained in a narrow range on the increasing of current from the minimum to the maximum limit. The aforementioned deviation of the inverter voltage from the rated value, which is dependent upon the number of converter groups in operation, represents one particular feature of current control performed by the inverter tap-changer control. The inverter control system also has the task of maintaining the DC line voltage constant for any value of current. This operation is accomplished by two voltage control systems; the minimum γ extinction angle regulator (see Chapter 4) which by regulating the extinction angle γ, holds the factor $\cos\gamma$ constant and the inverter transformer tap-

changer control which in order to hold the inverter no-load voltage Udi constant (see Chapter 2.3) causes the change of transformer tap position on the variation of the network voltage and of the transmitted DC current.

As seen in Chapter 2 the DC voltage of an inverter bridge is given by

$$Ud \approx Udi.\cos\gamma$$

Ud is thus maintained constant by the action of both the aforementioned control systems.

3.3 Converter Characteristics and Determination of DC Transmission Working Points

From what has been said in the previous chapter, a HVDC link operates at definite values of current and voltage under the combined action of the rectifier and inverter automatic controls. The working conditions of an HVDC system may therefore be described by curves, which are obtainable from the crossings of the rectifier and inverter control characteristics (Fig. 3.5a, 3.5b). In Fig. 3.6, these characteristics are combined. Their crossing point A represents the actual working point of an HVDC transmission scheme. The crossing point A can be shifted horizontally by the rectifier current regulator (constant voltage) within the permissible current range, or shifted vertically in a limited fashion (constant current) by the inverter transformer tap-changer.

In the prevailing working condition, the almost horizontal lines $\alpha = \alpha_o$ and $\gamma = \gamma_o$ represent the highest voltages that can be supplied to the DC line by the rectifier and the inverter respectively.

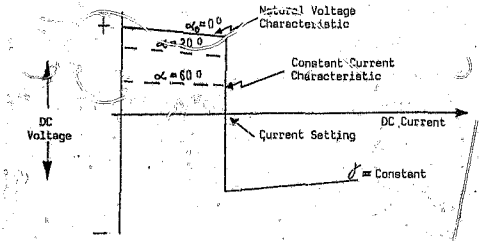


Fig. 3.5a Rectifier Characteristic

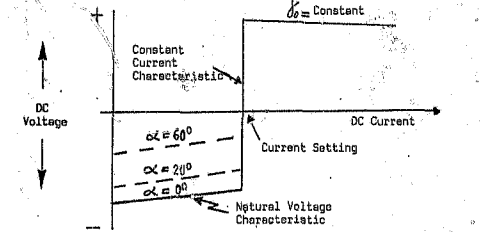


Fig. 3.5b Inverter Characteristic

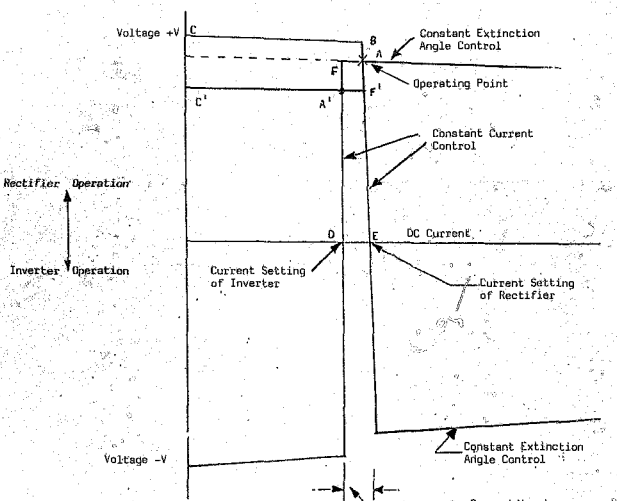


Fig. 3.6 The Classical Characteristics.

Normally the maximum rectifier voltage corresponds to a fixed firing delay angle (α = 16° in Songo), but as mentioned previously, a variation margin of α_0 is provided in order to vary the maximum rectifier voltage as fast as possible (α min = 13°, α max = 19°) (see paragraph 3.2).

The maximum voltage supplied by the rectifier can be rapidly varied by holding constant the current transmission as far as possible, expecially when sudden inverter voltage changes of limited amount are taking place. In other words, as can be seen in Fig. 3.6, the voltage difference between the rectifier and inverter, represented by the segment BA, is kept constant only by the fast action of the current controller, if the inverter voltage changes do not exceed a percentage of the rated value, approximately equal to voltage variation represented by a tap-changer step. At Songo and Apollo a tap-changer step represents a 1.23% variation of rated AC voltage value.

If the network voltage variation at the inverter exceeds the aforementioned voltage percentage, the action of the rectifier current controller precedes the slow performance of the tap changer control, (see paragraph 3.6) which in that case causes the tap-changers to run towards one of two extreme positions (steps 1 and 27 respectively), until the voltage balance required to keep the nominal line current steady, is again re-established (see paragraphs 3.4, 3.5).

Also during line re-energization, the fast action of the rectifier current controller in changing α in proximity of nominal value α_0 aids the DC system to rapidly reach the full load condition (Uhlmann, 1975a)

The DC inverter voltage, as illustrated in Fig. 3.5b is held constant at its maximum value for any current trans-

mitted by the rectifier current controller.

The inverter voltage is held constant by the constant γ automatic controllers with the aid of the inverter transformer tap-changers.

The constant γ regulator is a real-time processor (see Chapter 4), which computes the firing angle of each inverter bridge valve by regulating γ extinction angle at a fixed value (18° in Apollo). The firing angle is synchronized with the alternating line to line voltage, detected at the network side by means of measurement transformers (VTs) in order to obtain pure sinusoidal voltages in the synchronizing circuits of the firing controller. Fig. 3.7 illustrates the transformer line to line voltage replica and the advanced firing angle as they appear on the oscilloscope.

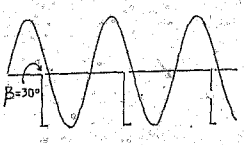


Fig. 3.7 Line to line voltage synchronized with firing pulses.

Since γ can be regarded as a time in agreement with the $\gamma = \omega t$, it is possible to say that the real-time processor of an inverter bridge determines the optimum time for firing the valves before the commutating voltage across the valves reverses. In performing this important task, the γ regulator must

(a) constantly analyse the commutating voltage peaks, the commutation inductance Lc, the value of the actual DC current;

(b) measure the actual γ of the outgoing valve and memorise it after each valve firing;

(c) select the minimum of the 6 memorised γ values at the end of any firing cycle (see paragraph 4.3.1);

(d) compare the selected γ with the reference value γ_n. A corrective actions on the valve firing times of the next firing cycle are carried out only at the end of these operations;

The relation

$$\cos \gamma_n = \cos\omega t + 2XcId / \Im Em$$

(Kimbark, 1971b)

correlates all the quantities involved [illegible] real-time processing of a γ regulator. It can be al[illegible]

$$\cos\omega t + 2XcId / \Im Em = \text{const}$$

since γ_n is held constant by the automatic regulator.

Considering 2Xcld / 3Em constant in time, the firing time of the valve is computed as a function of the choosen γ_n.

Furthermore from

$$Ud = Udi \cos \gamma_n - RcId*$$

which gives the relationship between the line DC voltage Ud and the γ_n extinction angle. Ud appears to be almost constant if $\cos \gamma_n$ and Udi are held constant.

* The above relation has been given approximately in Chapter 2, without considering the c.c.d. due to the negative equivalent commutation resistance Rc of the inverter.

3.4 Voltage Drop at Rectifier Station - Current Control by the Inverter Real-Time Processor

The almost vertical segment FD of the inverter characteristic in Fig. 3.6 represents the control action, performed by the inverter automatic control on the system current. In the normal working condition (steady-state) the automatic control at inverter side is essentially directed to keep the inverter output voltage at the rated value by regulating the γ extinction angles for each bridge. When the system current drops 10% of the rated value, the γ extinction controllers are taken out of inverter voltage control and are replaced by the inverter current controller (see paragraph 3.9.2) which, in the same manner as the rectifier Id controller, exerts a common control action on all inverters of a pole. Such action consists of a fast increase of the advance firing angle β in order to decrease the pole voltage as soon as possible, thereby avoiding the collapse of the current flow.

DC line current drop is due mostly to a rectifier voltage drop; that is, a collapse of rectifier voltage under the inverter voltage maximum level. *

In Fig. 3.6 the control of system current is taken by the inverter Id controller. Fig. 3.6 also shows the new rectifier voltage C'A' after having dropped from the primary level (segment C B') obtained this time by the crossing of the inverter current control and the rectifier voltage control characteristics respectively. It is clear that the inverter Id controller taking over the current control prevents the sudden collapse of power transmission, which however decreases proportionally to the voltage drop, with the current kept almost constant. Also the rectifier automatic control reacts to the rectifier voltage drop by

* Note: The inverter voltage maximum level is that at the minimum possible current transmission.

rapidly increasing the voltage at the rectifier output. The Id-controller can only increase the rectifier voltage up to a certain amount, and the task of increasing it further is performed by the rectifier tap-changer control.

In conclusion, the combined performance of the aforementioned control systems causes a new lower voltage balance between the rectifier and inverter groups, but the continuity of the rated current transmission is maintained.

With the help of the oscillograms of Fig.3.8 recorded at Apollo inverter station, we can see the inverter voltages (oscillogram 1;3;5;7e) and the line voltage (oscillogram d) decreased by the action of the inverter Id controller, resulting from a sudden voltage drop at rectifier side due to a bridge loss. The outage ot the rectifier represents a 25% loss of the total rated pole voltage at the rectifier side with 4 converter groups in operation (one pole); and to keep the original voltage balance between the two line ends, the line voltage at the inverter side should also be decreased by the same amount. This means that the output voltage of each of the 4 inverter bridges has to be decreased by 25% to get a total line voltage drop at the inverter end counterbalancing the voltage drop at the rectifier side. Taking into account that the action of the rectifier current controller can raise the pole voltage with the remaining three bridges in operation a 50% of the voltage drop by shifting the firing angle α to its permissible minimum (9°) , a decrease of about only 10% on the voltage of each inverter bridge, will lead to satisfactory voltage balance between the inverter and rectifier station so as to guarantee the flowing of current, though reduced by the same percentage.

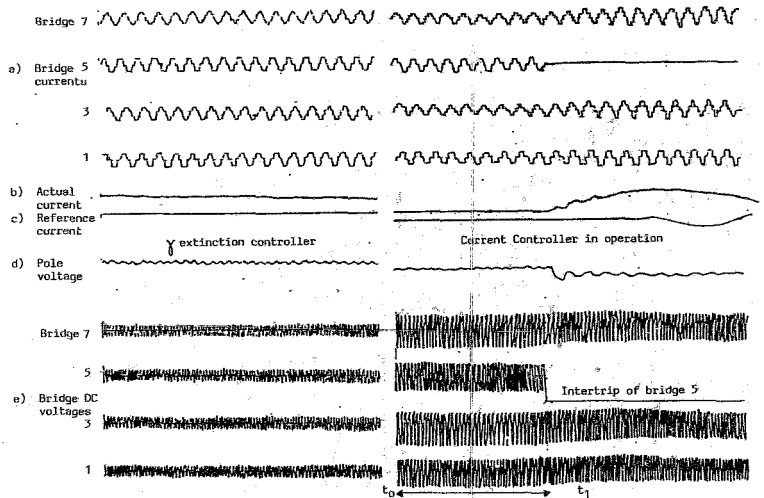


Fig. 3.8 *Inverter oscillograms (recorded at Apollo) to show the control of the γ-extinction controller and the current controller respectively.*

In the oscillograms of Fig. 3.8 the time interval t_0-t_1 is related to the performance of the inverter Id controller. Due to a bigger β firing angle there is a substantial increase of the bridge voltage ripple (*oscillograms e*), and the lower power transmission factor and electrical stresses on the inverter valves make such a feature of the automatic control objectionable for a continuous power transmission. If, therefore the duration of the rectifier voltage drop is thought to be dangerously longer than an established time (10 a in Apollo) due to a rectifier bridge outage, then an intertrip function issued via the PLC * system by the rectifier monitoring equipment will cause a bridge outage (instant t_1 in Fig. 3.8) at the inverter side and the automatic controls at both stations will very soon resume their normal type of operations at a lower line voltage level (oscillogram d in Fig. 3.8). It is important to note that, from that hitherto said, in the steady-state the rectifier and inverter control systems operate independently. This occurrence of an abnormal situation such as the rectifier voltage drop unifies and combines their control action to maintain as far as possible transmission of power. The rectifier and the inverter automatic control are linked by:

(a) the current command or the reference current signal transmitted to the inverter automatic control by the rectifier measuring equipment (see paragraph 3.9)

(b) the reference voltage signal transmitted by the inverted measuring equipment to the rectifier control (Kimbark, 1971c).

3.5 Voltage Drops at the Inverter Station

* Power line carrier

In the case of reduced inverter output voltage due to a drop of alternating voltage or because of a fault in the firing control of some bridges, the inverter characteristic (Fig. 3.6) is shifted downward. The current remains at the same level, but the power is reduced proportionally to the inverter voltage reduction. In fact, in consequence of the inverter voltage drop, the system current tends to increase; but it is prevented from doing so by the current controller at rectifier side, which causes the rectifier output voltage to decrease, by igniting the bridge valves with a bigger firing delay angle α. The automatic control of the inverter can rapidly recover the drop in voltage if such a drop does not exceed 2% of the rated inverter voltage value. Theoretically the extinction angle controller (see Chapter 4, paragraph 3.2) could restore a 6% of the voltage rated value, if the aforementioned γ controllers were free to fire the valves with a smaller advanced firing angle on the occurrence of inverter voltage drop. But a solution of such a nature leads to dangerously decrease the γ angle, which must be maintained at such a value (18° at Apollo) as to guarantee a safety gap in respect of the minimum angle (9° for thyristor valves) at which the inverter operations might be jeopadized by commutation failures (see Chapter 5). If the amount of the voltage drop is bigger than 1,2% of the inverter voltage rated value, the inverter tap-changer control will operate after a certain delay and voltages for an extent (27 - No) 1,2% of the rated value may be restored. No represents the maximum number of steps that the tap-changers have to run before reaching the highest step 27, which gives the maximum voltage ratio in the inverter transformers. Also at the rectifier side, the tap-changers will run towards such a position to guarantee a constant flowing current as soon as the delay angle α reaches 19° (see paragraph 3.2).

In case of the loss of one inverter bridge or more, the amount of voltage drop is relevant and cannot be always recovered by the automatic firing and tap-changer control. Moreover conditions in which the rectifier valves are fired with very big delay angle are to be avoided due to rise of dangerous harmonics in the AC rectifier network (stresses on the AC filters) and also in the DC line side (stresses on the DC filters), and due to the possibility of discontinuity in current transmission. So that a new lower voltage balance between the two stations has again to be considered; as usual an intertrip signal (carrier transmission) or a manual trip of an equal number of bridges at rectifier side will restore a lower voltage balance. Fig. 3.9 shows the line voltage drop (oscillogram d) due to an inverter bridge loss and the temporary increase of the system current (oscillogram b) immediately restrained by the rectifier current controller (oscillogram c).

3.6 Tap-changer Control at the Rectifier and Inverter Stations

Paragraph 3.2 states that at the rectifier side, the tap-changer control has the task of maintaining in the steady-state the firing delay angle α within a limited range, and that because a change of the delay angle implies a change of the rectifier DC output voltage and consequently a variation of the DC transmission (see paragraph 3.7.2) capacity although the power demand setting is unchanged. Fig. 3.10a shows the control of the tap-changer at Songo substation for one converter group in operation and for the maximum direct current transmission (Id = 1 800 A), with variations of the AC system voltage not exceeding 10% of the nominal value (220 kV). For example, the steady working condition with AC voltage at its nominal value (220kV), the firing angle α = 16° and the tap-changer in position 17, a 5% drop of the AC voltage from the nominal

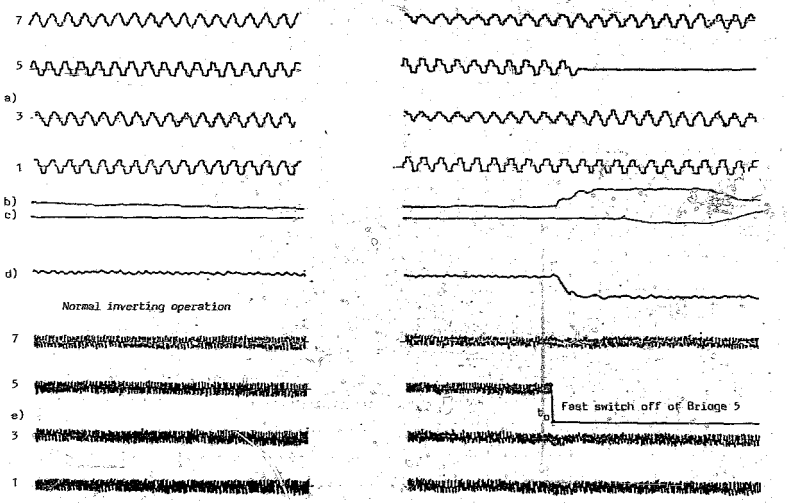


Fig. 3.9 Records of line voltage drop (d) and system current increase due to loss of an inverter.

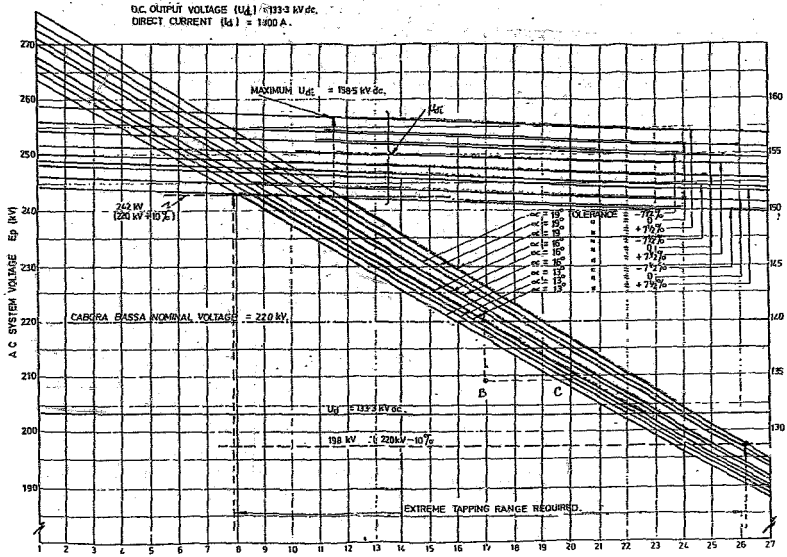


Fig. 3.10a Variation of E_p and U_{do} with tap position (rectifier)

CABORA BASSA D.C. OUTPUT VOLTAGE (U_d) 133·3 kVdc.
EXTINCTION ANGLE γ = 18°.
LINE DIRECT CURRENT AT CABORA BASSA: (I_d) = 360A, 1800A, 3300A.

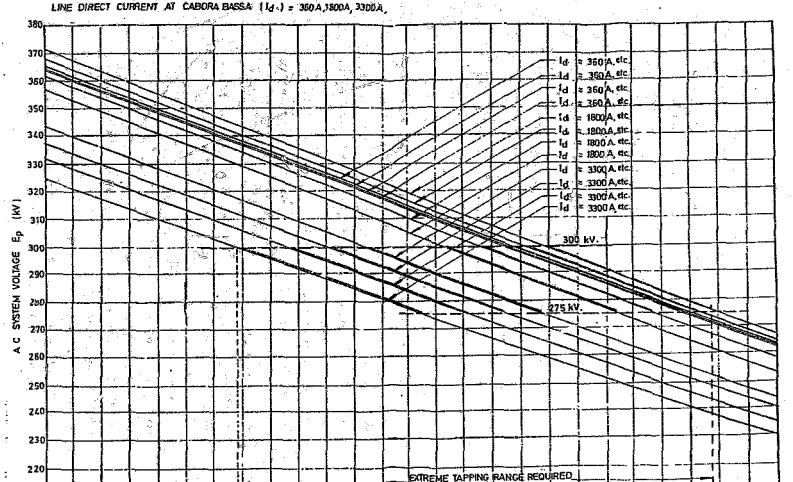


Fig. 3.10b Variation of AC System Voltage with tap position (inverter)

value represented by point B in Fig. 10a causes the tap-changer control to shift the taps to position 20 in order to restore the deviation of the firing delay angle within the range permitted (13° - 19°) in the steady-state condition (point C). It must be noted that the same graph of Fig. 10a shows that to keep the DC output voltage constant in the steady-state, the tap-changer control shifts the position of taps to vary the no-load voltage Udi within a certain range. When the drop in AC voltage exceeds 10% of the nominal value a bigger firing delay angle has to be set by the rectifier control depending on the decreased capacity of the generators.

It is clear that the DC output voltage would be decreased and the DC transmission reduced.

The tap-changer control steps the taps towards the position which makes the DC output voltage capable of transmitting the maximum possible current at a lower level of generation. (No-load voltage (see Chapter 2) adjustment by tap-changer control).

The inverter tap-changer helps the real-time processor (γ extinction angle controllers) to maintain the DC voltage constant for any current transmitted by the rectifier station. Fig. 10b shows graphically that the inverter tap-changer controller moves the taps upwards or downwards to keep the DC inverter voltages at a fixed value for any transmitted current (voltage regulation by inverter tap-changer control).

When the inverter Id controller takes over on the firing control of the bridge valves, the inverter tap-changer steps down the taps for lowering the firing angle β and consequently the γ extinction angle. This operation is

necessary to keep the power factor ($\cos \gamma$), within acceptable limits. (γ extinction angle decreased by the inverse tap-changer control).

3.6.1 Tap-changer Controller

Fig. 3.11 is a block schematic diagram of the transformer tap controller in use at Songo and Apollo.

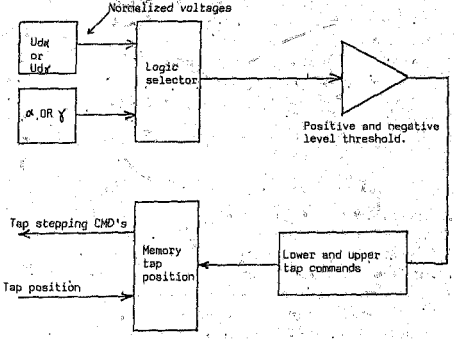


Fig. 3.11 Tap Controller block diagram.

The pole voltage is given a nominal value to make the tap-changer control system independent of the number of the switched-on bridges or from the pole voltage. The logic selector provides the interlock of the two operating modes described in

paragraph 3.6 for both terminals.

The positive and negative threshold circuit has two outputs; one for lowering and the other for raising the tap-changer position. The threshold circuit is adjusted to give an output for an AC voltage variation of about 1.23%. The adjustment is made in such a way as to avoid oscillations of the tap-changer from a position to the adjacent one. In other words, the threshold must output its command when a certain dead band is overridden. The dead band has been established as being between 1,5 to 2 tap steps (Zamco TSE, 1971).

3.7 Power Control

3.7.1 General

The flowing of power from the AC generators to the DC system through the converter bridges (rectifiers) is regulated by sophisticated electronic devices, which have the main task of maintaining the continuity of power transmission in the steady-state and also during power changing conditions. An electronic system designed to control the power flow must therefore be capable of

(a) maintaining the AC frequency of the busbar at the generation plant within the restrained band (in Songo substation 49,7 - 50,3 Hz) and reasonably limited (in Songo 57 Hz) when load is rejected by HVDC transmission;

(b) changing the rate of AC and DC power as much as possible by a direct control of the generator

outputs and the DC load transmission respectively.

(c) maintaining transmission reliability and availability capacity

(d) and finally co-ordinating the operations needed for power transmission between the power station and DC links.

The foregoing are fundamental requirements to ensure the total AC generated power conversion into DC power and its transmission to the inverter end, under any working condition (Kimbark, 1971d).

Some of the aforementioned requirements, however are not always satisfactorily achieved during very fast transients and in the event of load rejection by the DC transmission. This is mainly because the power controller is limited on the performance of particular tasks (as for instance rapid and adequate rate of power changes at the generator outputs in relation to the speed of change of DC power) by several factors related to the type and duration of the disturbance and to very different time constants of the systems under control (see Chapter 5, paragraph 5). Consequently during load rejections there is the possibility of the occurrence of AC frequency changes making the tripping of the AC filters unavoidable. Furthermore, the tripping of some generators is to be expected when the unbounded increase of Kinetic energy raises the frequency enormously and puts the generators under stress.

3.7.2 Master Power Controller at the Rectifier Substation

The system for the control of power flow at Songo substation is named Master Power Controller (MPC) and can be schematically represented by the block diagram of Fig. 3.12. Two main functions are generated by the MPC to control the power flow: the command (PO1 and PO2) to the controllable generators (the controllable generators are those allocated to a particular DC pole and receive a power order directly from the MPC) and the other (PN1 and PN2) to the DC pole control. Both are derived by the actual power transmitted signal (PC1 and PC2) at the output of the power demand distribution module as result of the actual power demand setting and the actual DC pole power capacity calculation.

(a) Power Capacity of a DC Pole

The determination of power capacity or the maximum possible power of the DC pole, is calculated by multiplying the selected minimum of the following functions:

(i) Maximum possible load = 0

(ii) Idref (Current control see paragraph 3.8) set value derived by the power order (NP1 and NP2) to the DC control

(iii) Idref = 0 from the various protection circuits

(iv) Idref = Idn, the nominal maximum direct current (1 800 A) used to determine the "max possible power"

with the pole voltage (see Chapter 2 paragraph 5).

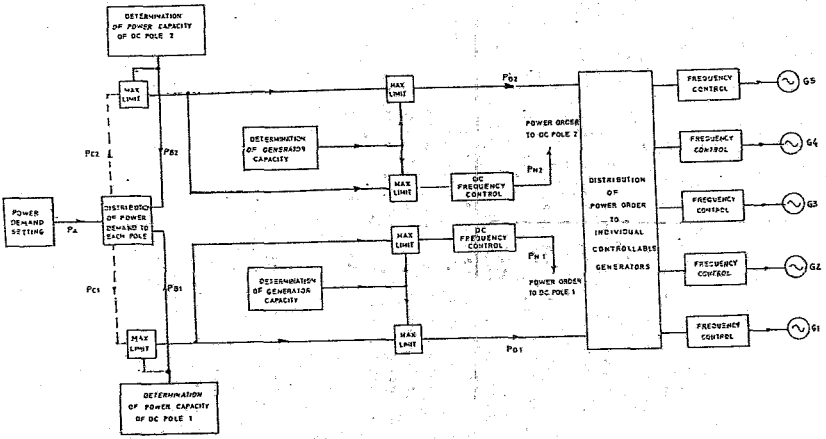


Fig. 3.12 Simplified schematic diagram of the Master Power Controller at rectifier station (Songo)

(b) Frequency Control in Steady Condition

The measured AC frequency on the busbars is led to two M^C modules which are controlling the system frequency by varying the power order (PN1 and PN2) to the DC load, and by modulating the power order (PO1 and PO2) to each individual generator respectively. The module used to control the frequency through the power order to the DC load, operates when the frequency exceeds a certain limit (± 0,2 Hz) by altering the DC transmission rapidly.

When the stepping up or down of the power causes large variations in frequency, its control is performed by both modules. Since the power delivered by the generators can be changed slowly, the rate of change of the power order to the DC transmission must be properly adjusted, to get a smooth increase or decrease of power transmission (Calverley, 1972).

3.7.3 Control of Frequency on DC Load Rejection

In the event of DC load rejection (50% rejection for a persistent fault on one line, or 100% rejection for a persistent fault on both lines) one or more control frequency modules will intervene and compute the surplus generator capacity due to the loss of a pole or two poles, and will trip sufficient generators to retain the frequency rise to approximately 57 Hz (see Chapter 5, 50% load rejection at Songo due to a line fault).

3.8 Current Reference and Actual Current

The reference current is a function originated in the rectifier automatic control by dividing the power order to the DC transmission with the actual pole voltage (see block diagram Fig. 3.13).

The reference current represents the current which at any instant is to be transmitted for satisfying the two requirements of total power demand * and the maximum possible power. The actual system current is the transmitted current which follows the variation of the reference current through the feedback process of the rectifier current controller, whose output gives the error functions used to create the firing conditions for the valves.

The reference current is transmitted via the Power Line Carrier to the inverter automatic control, which in turn memorises and uses it to control the flowing of current when a consistent rectifier voltage drop occurs (see paragraph 3.4). But in order to obtain separate actions for the rectifier and for the inverter current controller in regulating the system current, the reference current received by the inverter automatic control is decreased by a certain ΔI_d. In the classical DC characteristic of Fig. 3.6, such a current margin is represented by the segment DE on the horizontal axis. We can conclude that the inverter current controller is activated when the system current drops to a value $I_d - \Delta I_d$. As we said in the foregoing, the rated value of current transmitted from Songo, being around 1 800 A, a current decrease ΔI_d equal to 10% (180A) of the rated value will activate the Apollo current controller.

3.8.1 Current Reference Limits and Permissible Rate of Change

* The total power demand is the power required by the inverter end, limited by the maximum possible power available.

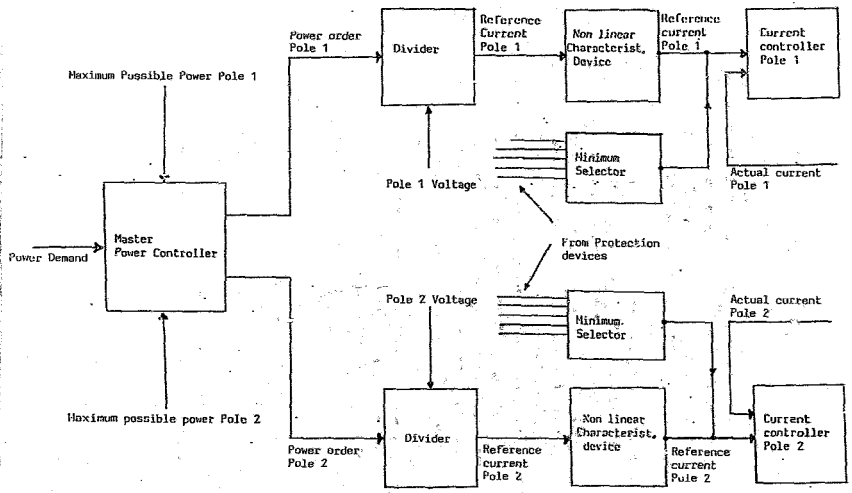


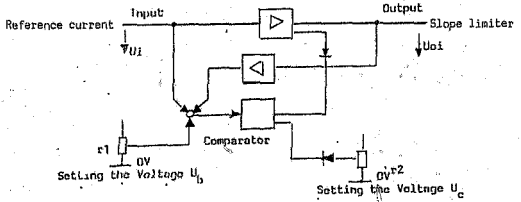
Fig 3.13 Schematic block diagram of the generation and control of the *reference currents at rectifier station* (Songo)

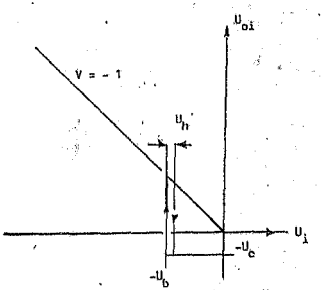
It is very important to ensure that the reference current function does not exceed a maximum (upper current limit) because of the possibility of thermal damage to the valves or to the line, when line faults occur, by the actual current. (In the Songo - Apollo scheme, the upper current limit is 1,25 times the rated current 1 800 A).

Moreover a minimum current limit is also determined by an electronic device operating before the reference current input of the rectifier current controller. As illustrated in Fig. 3.14, such a device has a transfer function that is linear from a fixed minimum value of current (360 A in Sonyo), and varies with a maximum permissible rate of change. Such characteristic does not allow the raising of intermittent current, especially when the rectifier valves are fired with the biggest delay angle (low current). The limitation of the positive rate of change of current is to be considered in relation to the protection of various parts of the plant, and for this reason the positive rate of change is controlled by the value of the main voltage (three-phase supply network).

Fig. 3.15 illustrates the second stage of the device limiting the rate of change of the reference input. When a sudden positive change of the reference current Uoi* occurs at a certain instant t_0, the final value of the reference input Uo is reached after a delay time $t_3 - t_0$, and a very short delay time is foreseen in case of a sudden negative change of the reference current (instant t_5).

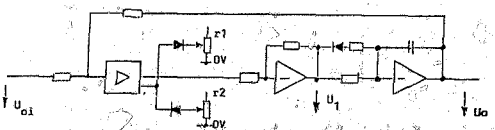
* Uoi is the voltage representing the Idref function.





for $U_i \leqslant -U_b$ and $U_i < 0 \Longrightarrow U_{oi} = -U_i$

Fig. 3.14 Non linear operating characteristics of the device to influence the reference input of the current control circuit (Songo)



Basic structure of the slope limiter at current controller input

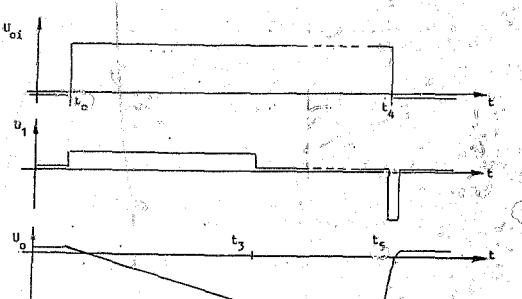


Fig. 3.15 Limitation of the rate of chenge of the reference *current input* at *rectifier* current controller by the slope limiter (Zemco TSE, 1979).

3.8.2 Reduction of the Current Limits

In order to protect the several parts and equipment of the plant, which might be seriously damaged on the occurrence of failures, the DC current may be reduced by means of protective and monitoring devices.

The following Table gives a schematic description of the lower limits of the DC current, when particular disturbances occur.

(a) Current limit reduced to 0,3 X IdN due to:

(i) Commutation failure of the inverter (see Chapter 5).

(ii) Voltage dependant current reduction from the inverter station. (see Chapter 5).

(b) Current limit reduced to 0,4 X IdN due to:

(i) 50 Hz in the pole voltage detected by the rectifier state protection device

(ii) Voltage dependent current reduction from the rectifier station protection

(c) Current limit reduced to 0 X IdN due to:

(i) Manual commands from the control rooms of both stations

(ii) Pole differential protection (see

Chapter 5).

(iii) Firing monitoring (see Chapter 5) from the inverter station

(iv) F = 68 Hz (599 kVA). The frequency of the power supply system (first grade) is less than, or equal to, 68 Hz

(v) Undervoltage in 3-phase system U1< 0,5 ULN (from Songo)

(vi) A drop in the pole voltage for t> 1 sec, caused by the commutation failure of one converter bridge, and measured by the voltage-dependent current limit reduction detector at the rectifier station. (Ud < 0,5 ULN, t > 1 sec)

(vii) A fault on the DC line, sensed by the line protection detector at the rectifier station, which provides also the restart of power transmission after a delay from the fault occurrence (see Chapter 5, paragraph 2.8)

The 0,3 X IdN and the 0 X IdN command signals originated in the inverter station are transmitted via the telecommunication system to the minimum reference current selector, which selects the reference current for the input of the rectifier Id controller (see block diagram of Fig. 3.13)

3.9 Current Controller

3.9.1 Current and Voltage Controllers at Rectifier Station

The signal current reference originated by dividing the power reference from the MPC by the pole voltage is an input of the rectifier current regulator. The other input is the function to be regulated, that is, the actual system current (paragraph 3.8). The current controller has been designed with the aim of having a "continuous safety control", and two current regulators therefore are used in parallel. A selective circuit chooses the minimum between the two regulator outputs, and only the one with the smallest output regulates the current. More precisely the selective circuit selects among three signals - the output of the rectifier voltage controller is also selected for the control of rectifier valve firing as soon as the direct output voltage Ud exceeds a prefixed limit.

It can be said that the voltage controller represents a protective circuit against the overvoltages which may occur when the delay angle α reaches values beyond the minimum allowed (9° at Songo). It is necessary to emphasize that the delay angle α is blocked from going beyond its minimum by means of limiting potentiometers at the outputs of the current controllers and also at each bridge voltage control output (see block diagram of Fig. 3.18). That, however, does not eliminate the possibility of the shifting of the firing below the minimum because of disturbances or failure of circuit components.

Paragraph 3.2 states that at the maximum load, the firing angle can assume a value of 13° to 19°. This corresponds to a current regulator output which independent of the operating bridge number ensures the maximum permissible power transmission (maximum current). It is possible that a sudden

temporary drop of the rectifier output voltage would cause the load current to decrease (more than 10%). The current regulator then forces the delay angle towards its minimum (9°) in attempt to recover the voltage loss. In this case the rectifier current regulator acts as a direct voltage controller and obviously the control of current is taken by the inverter current controller (see paragraph 3.9.2). It is clear that in this manner the direct voltage at the output of rectifier will be kept constant by the rectifier current controller until the direct voltage is restored (paragraph 3.4).

From block diagram Fig. 3.16 the rectifier current controller output or the error function is

$$\varepsilon = I_r - I_a$$

where I_r represents the reference current, and I_a is the actual value of the DC current.

The transfer function of the current controller is made non-linear (Fig. 3.17), to get different response for errors falling within different ranges. The reason for that is to provide stability of the DC transmission during steady conditions (lowest error value) and to increase the flexibility of the control during the transient (highest error value) Because however, of the non-linear effect on the delay angle α, which depends on the current controller output error, a corrective circuit (Fig. 3.18) at the output of current controller compensates properly the error function in order to get a linear α and consequently a linear control of direct output voltage ($\frac{d\ Ud}{d\ Udi}$ = const.)

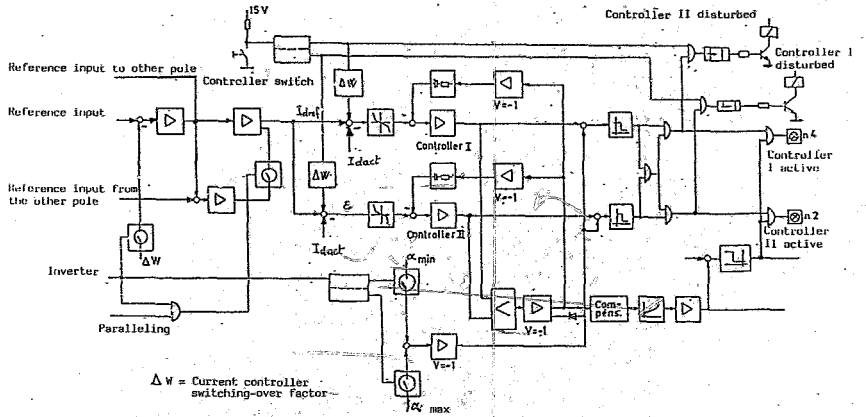
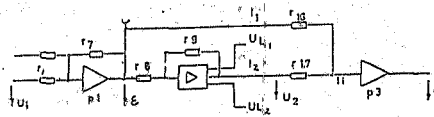


Fig. 3.16 Block diagram of the current controller (Zamco TSE, 1979).



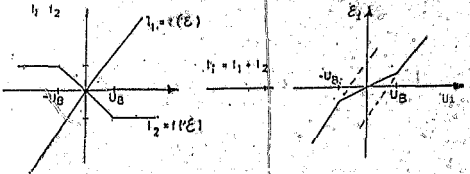
ε_1 = Control error

$I_t = I_1 + I_2$

$I_1 = \frac{\varepsilon}{r16}$ and for $U_{L2} < U_2 < U_{L1} \Longrightarrow I_2 = -\frac{r9}{r8\ r17}$

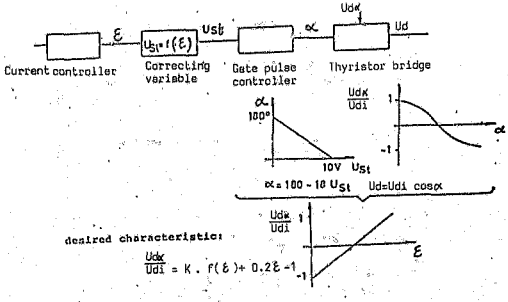
for $U_2 = U_{L2} < 0 \Longrightarrow I_2 = -\frac{U_{L2}}{r17} = \text{const.}$

for $U_2 = U_{L1} > 0 \Longrightarrow I_2 = \frac{U_{L1}}{r17} = \text{const.}$



U_B can be adjusted via voltage UL1
U_B can be adjusted via voltage UL2

Fig. 5.17 Non linear characteristic of the current controller



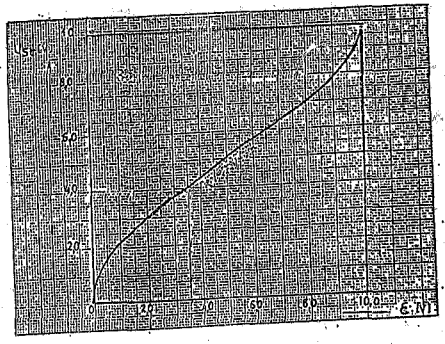


Fig. 3.18 Operating characteristic of the corrective variable Ust (Zamco TSE, 1979).

3.9.2 Current Controller at Inverter Station

The inverter station current controller does not differ substantially from the one at the rectifier station

The error function is given this time by

$$\varepsilon = I_r - \Delta I_r - I_d$$

The reference value is now $I_r - \Delta I_r$ for the reasons described in paragraph 3.8.

When the error is negative, the control for the firing of the valves is performed by the γ extinction controller (Chapter 4). When the error becomes positive the inverter current control takes over the control of firing angle β for reducing the direct output voltage (current control by the inverter).

3.10 Firing Pulse Spacing Control

Providing the firing of valves at the same time interval (3,3ms corresponding to 60°) is a very important task, which has to be carried out by the automatic control at the rectifier as well as at inverter station. The presence of harmonics in the commutation voltages causes the 6 valves of a bridge to be ignited at different intervals of time. This generates abnormal or uncharacteristic harmonics* that must be suppressed or decreased,

- firstly to avoid disturbances and interferences on the telephone lines, and
- secondly in order to diminish the risk of instability, which might affect the entire system when the uncharacteristic harmonics interact with the characteristic ones, originated by the convertors during the valve commutations.

* They are originated when the ignition times of valves are alternately late and early.

Different methods to implement the accuracy of firing intervals have been developed, mainly based on the individual phase and equidistant control principles. The use of digital circuits along the entire firing control chain has also been suggested. This would also improve the stability of the firing pulses in respect to drifting effects. In the Songo rectifier station and in the Apollo inverter station the firing pulse spacing is ruled by several technical expedients that contribute to maintain the variation of pulse intervals to within acceptable tolerances (0,1°).

Probable harmonics on the synchronous voltages are removed by the use of active filters at receiving ends of signal repeater transformers and at steady working condition, very highly stabilized 300 Hz generators provide accurately spaced pulses to the input of ring counter digital circuits. The unavoidable distortions which affect the firing pulses during their journey towards the valves (presence of non-linear components and apparatus such as pulse transformers and fibre optic transmitters and receivers) are suppressed by rebuilding and re-spacing the distorted pulses. These operations are performed by digital processors (command units) located close to the valve firing gate amplifiers. (Uhlmann, 1975b).

SUMMARY

Chapter 3 stresses the importance of a control device for the supervision of a DC transmission link, not only to ensure stable transmission of the DC power, but also to cope with unpredicable events such as power fluctuations. The control device is necessary because information on these events is not available from the AC network to initiate control actions on the DC power to be transmitted over the link.

The use of the direct current and DC line voltage as primary control parameters to avoid major consequences resulting from minor voltage variations on the two interconnected networks, is described. The limiting of the current by the current controller for valve protection (highest limit) and for avoiding disruption of power flow (lowest limit), is also described.

Finally, the control system is dissected into its basic functional elements which perform independent as well as combined actions at the rectifier and inverter stations to prevent undesirable fluctuations and instability thus ensuring steady power transmission.

References

1. Calverley T.E. (1972) Operation of Cahora Bassa generating station and HVDC transmission at Apollo, Report TEC/2418/261072A, pp. 2-9.

2. Kimbark E.W. (1971a) Direct current transmission, 1st ed. New York: Wiley, 1971, vol. 1, pp. 148-183.

3. Kimbark E.W. (1971b) Direct current transmission, 1st ed. New York: Wiley, 1971, vol. 1, pp. 167-172.

4. Kimbark E.W. (1971c) Direct current transmission, 1st ed. New York: Wiley, 1971, vol. 1, pp. 158-162.

5. Kimbark E.W. (1971d) Direct current transmission 1st ed. New York: Wiley, 1971, vol. 1, pp. 180-183.

6. Reeve J. et al. (1972) An automatic control scheme for [illegible] transmission using digital techniques, Transaction [illegible] presented at IEEE Winter Meeting, New York, Feb. 1972, pp. 1-6.

7. Uhlmann E. (1975a) Power transmission by direct current, 1st ed. Berlin: Springer-Verlag, 1975, pp. 140-162.

8. Uhlmann E. (1975b) Power transmission by direct current, 1st ed. Berlin: Springer-Verlag, 1975, pp. 150-162.

9. Zamco TSE. (1971) Basic design of the HVDC station Cahora Bassa and Apollo, Report SS20/1 pp. 11-17.

10. Fig. 3.17 Zamco TSE, (1979) Station-half control cubicle, *Cahora bassa-Apollo document* No. 551/TSE-A60-BGB23, Apollo (IRENE, SA), 1979, sheet 3/18.

11. Fig. 3.18 Zamco TSE, (1979) Station-half control cubicle, Cahora Bassa-Apollo document No. 551/TSE-A60-BGB23, Apollo (IRENE, SA), 1979, sheet 5/11.

12. Fig. 3.18 Zamco TSE, (1979) Station-half control cubicle Cahora Bassa-Apollo document No. 551/TSE-A60-BGB23, Apollo (IRENE, SA), 1979, sheet 5/14.

CHAPTER 4

THE INVERTER AND ITS AUTOMATIC CONTROL

4.1 Introduction

The primary function of the inverter consists of transforming the DC current into a three-phase AC current synchronised with the network into which power is to be fed.

This can be only obtained by providing the inverter with a firing control system which fires the valves at equal intervals of one-sixth of a cycle (60°) and in synchronism with the network frequency.

Another important function which has to be accurately performed by the inverter control system is to maintain the DC line voltage constant for any value of current transmitted by the rectifier(see paragraph 3.3).

In addition, the inverter control has to protect the valves and maintain continuity of power transmission by reacting to any variation of voltage and current originated by faults or transient conditions.

The controlling operations are carried out by real time signal processors, which may intervene at any instant to vary the firing of the bridge valves so as to change the electrical characteristics of the bridge itself to suit the actual operating conditions.

Fig. 4.1 and 4.2 show the inverter bridge operating in an HVDC system, the DC to AC current conversion caused by the controlled firing of the bridge valves, and the voltage across the valves during the firing process.

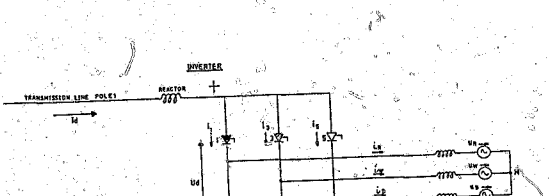
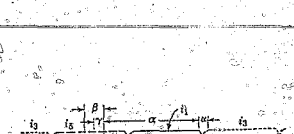


Fig. 4.1 Inverter bridge and the DC/AC current conversion.



$i_1 \ldots 6$ Valve currents

i_r, i_w, i_b output bridge currents

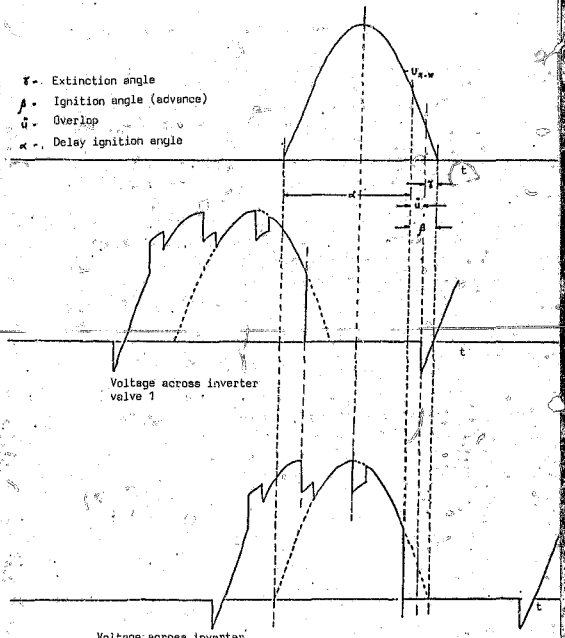


Fig. 4.2 Voltages across two inverter valves consecutively fired and the relevant angles of commutation.

4.2 Real Time Processors at the Inverter Station

The real time processor at Apollo is formed by the interconnection of four basic analogue circuits which determine the settings and the shift of the valve firing angle β through a common stage or voltage control block.

In the steady condition and from a minimum DC current of not less than 340 A, the control of firing is fundamentally due to the closed-loop γ extinction angle, which maintains the firing angle β constant by regulating the γ extinction angle of any valve to be fired. Regulating the γ extinction angle also maintains the bridge DC voltage at a constant value or at least within limits on the varying of transmitted current. (see Paragraph 3.2).

The shifting of the valve firing angle is carried out by the 90° ramp generator in conjunction with the bridge switching on and off, or for protection purposes, by 60° shifter in the event of commutation failure (see paragraph 5.1.5), or when the inverter valves are fired with a bigger angle (inverter current control) to decrease the inverter voltage to maintain the current flow when there is a drop in rectifier voltage.

The block diagram of the real time processor controlling the firing of an inverter is represented schematically in Fig. 4.3.

The output of the control voltage block is the controlled function which causes the network-synchronised pulses from the firing generator to fire the bridge valves with a firing angle β suitable for the actual working condition.

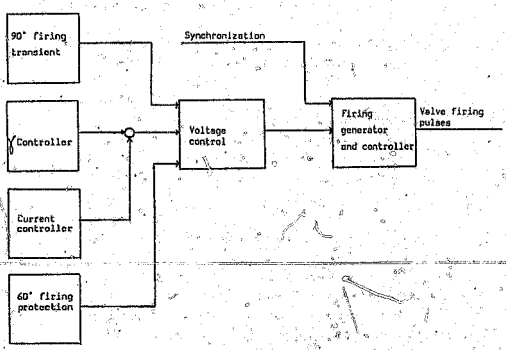


Fig. 4.3 Block diagram of the real time inverter processor. (Apollo).

4.3 The γ Extinction Control Loop at Inverter Station

Fig. 4.4 shows the block diagram of the γ regulator loop operating at the inverter bridge.

The various functional blocks forming the closed-control loop are partly situated indors and partly outdoors, and because the control and the protection signals are transfered to and from the bridge valves, they have to be shielded against the possibility of external disturbances.

Fig. 4.4 summerizes all functions carried out by the indoor control circuits, which will be discussed in the following paragraph (Zamco TSE, 1979a).

4.3.1 Indoors : General principles about the Error Function, Feedback and Control Elements of the Extinction Controller.

The function error ε is given by the difference between the actual value of γ selected as minimum among 6 γ angles measured for each bridge valve at any firing cycle and a predetermined reference value (18°).

$$\varepsilon = \gamma_a - \gamma_r \quad *$$

The selection of the minimum γ as actual value is based on the concept to form an error which can guarantee a safety margin as to fire the valve before the region of the possible commutation failure is reached (see Chapter 5). Considering the voltage across the valves as the controlled variable at the output of the γ control loop, a transducer is used as the feedback element required to establish a functional relationship between the actual γ and the valve voltages. The functions of the transducer are:

(a) to accurately measure the duration of the reverse voltage across each valve at each firing cycle;

(b) to transform these measurements into a series of 6 voltage quantities or levels;

* γ_a = actual , γ_r = reference

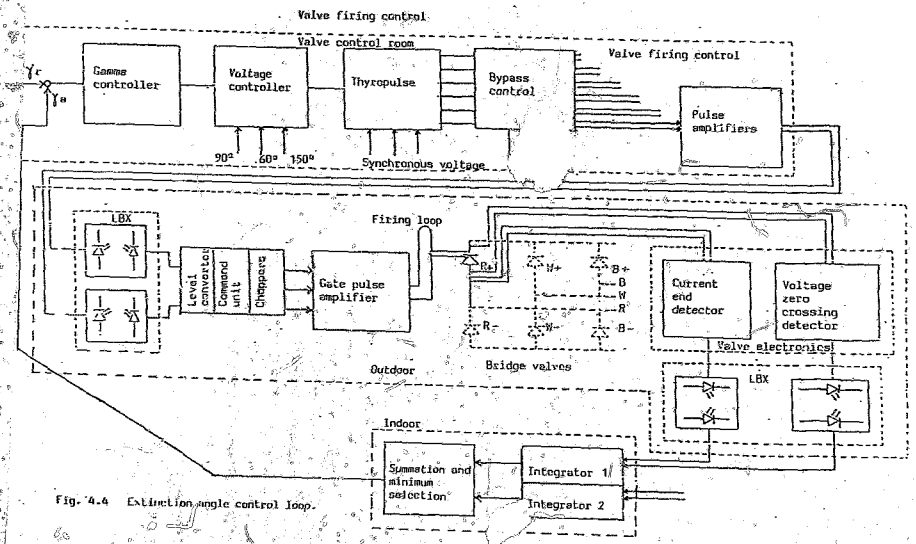


Fig. 4.4 Extinction angle control loop.

(c) to select the smallest of these levels, to get the actual value of γ needed to form the error for the setting of the new firing cycle (see paragraph 4.3.5).

The control element of the γ regulator consists of a succession of several devices which are required for:

(d) generating the appropriate control signals (see paragraph 4.3.3);

(e) transmitting the control signals through the bridge high voltage zone (see paragraph 4.3.4 and 4.6);

(f) reforming, checking and re-transforming the *control signals before they are applied to* the valve control gates. (see paragraph 4.6). (Muttelsee, 1969).

4.3.2 The γ controller and the error functions

(a) the error between the reference value and the γ minimum selected from the 6 actual values measured at each valve is calculated by means of an operational amplifier at the input of the γ control circuit. Considering the block schematic diagram of such circuit (Fig. 4.5), the errors $\gamma = \gamma_e - \gamma_r$ obtained are amplified differently by two blocks K_1 and K_2 in parallel in such a way that the new errors ε' will be

$$\varepsilon' = K_1 \varepsilon \quad \text{for} \quad \varepsilon < \varepsilon_K \qquad \text{UR}$$
$$\varepsilon' = K_2 \varepsilon \quad \text{for} \quad \varepsilon > \varepsilon_K$$

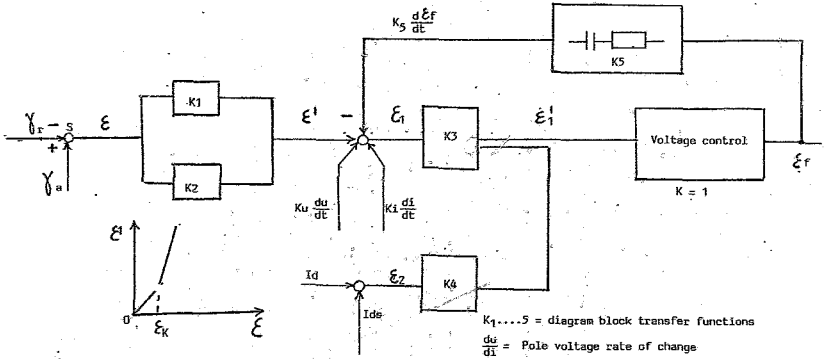


Fig. 4.5 γ-controller block diagram.

$K_1 \ldots 5$ = diagram block transfer functions

$\frac{du}{dt}$ = Pole voltage rate of change

$\frac{di}{dt}$ = Line current rate of change

$I_d s$ = minimum value of DC current allowed

This means that the entire block formed by the two K_1 and K_2 in parallel modifies the error transfer function from linear to exponential by combining two different error ramps (breaking point ε_K).

The block K_4 gives the command to transfer the error ε' to the output of K_3 when the difference $\varepsilon_2 = Id - Ids$ * is positive; that is to overstep the region of the intermittent currents.

In conclusion, the steady operation of the extinction angle controller is characterized by the equation: $\varepsilon_1 = K_3 \cdot \varepsilon_1'$, where K_3 can be considered constant and equal to one.

Disturbances due to the positive current rate of change, or due to the negative voltage ** rate of change over certain limits, modify the error calculated by the summator S and the paralleled blocks K_1 and K_2. ***

Therefore the general expression of the error at the γ controller output will be

$$\varepsilon_1' = K_3 \left(\varepsilon' - K_u \frac{du}{dt} + K_i \frac{di}{dt} + K_5 \frac{d\varepsilon'}{dt} \right)$$

for $Id > 0{,}25\ IdN$,

* NOTE 1: Ids represents the minimum value of current allowed for DC power transmission (360 A at Apollo)

** NOTE 2: Network voltage

*** NOTE 3: The negative voltage rate of change has been prevented from affecting the error functions at the Apollo controllers.

otherwise ε_i = constant (≈ 0,35 V) for any value of current less than 0,25 IdN. This means that the γ control loop is cut off from the valve firing process when the bridge is in operation and in the absence of DC current. In such a case the valves are fired under the control of the inverter current controller, whose output signal (- 1,7 V) for Id = Idref = 0 is selected as the minimum by the threshold selector (see Fig. 4.6). The minimum is selected from the signals at the outputs of the Id controller and γ-controller and is transferred through the control voltage block to the input of the trigger generator. When current flows, firing control is rapidly taken over again by the γ extinction control loop, which is allowed to extend the control of the valve firing β up to an angle with the smallest γ permitted. (The γ-controller generates the maximum error ε_i max (- 1,7 V))* The minimum error ε_i min (≈ 3,6 V) is normally reached in case of negative voltage rate of change du/dt and positive current rate of change di/dt. The two rates of change must exceed a certain limit before the threshold blocks Ku and Ki respectively cause the proper error correction to increase the firing angle β, in attempting to keep γ constant.

* **NOTE:** The error ε_i maximum must be limited to maintain a safe firing margin from the region in which extinction angle can become smaller than 9°, (recovery angle of the thyristors used at the Apollo bridges), and that to prevent the occurrence of valve commutation failures. (see paragraph 5.1.4).

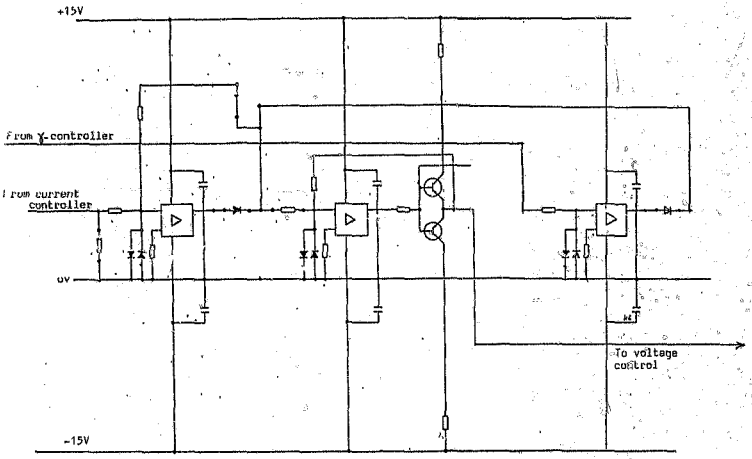


Fig. 4.6 γ-Controller-current controller threshold selector (Zamco TSE, 1979).

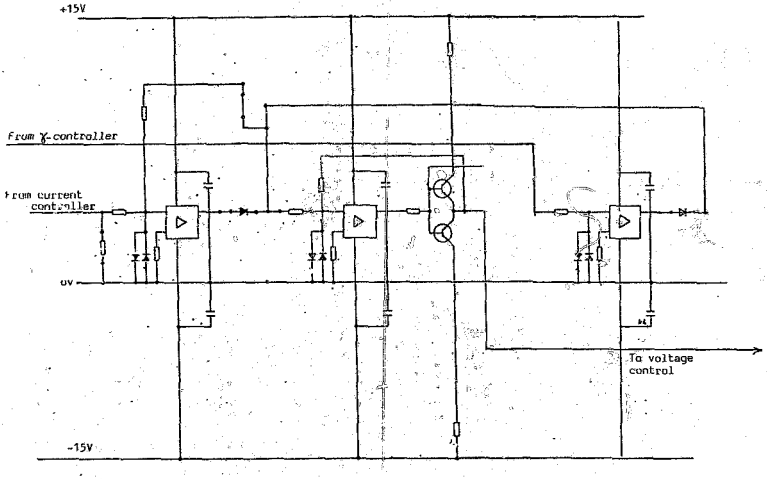


Fig. 4.6 γ-Controller-current controller threshold selector (Zamco TSE, 1979).

Nevertheless if the rate of change in current is very steep, commutation failure is bound to occur in some of the bridge valves, as discussed in Chapter 5, paragraph 1.4.

(b) Disturbances on the γ Control Loop

We consider now the block schematic diagram of the γ control loop, Fig. 4.7. It is possible that various types of disturbances may effect the output of the transducer as well as the input or output of the control voltage block. These disturbances may be originated by fluctuation of the amplifier operating points, sudden voltage peaks due to failing power supplies, magnetic fields, or merely electronic device failures.

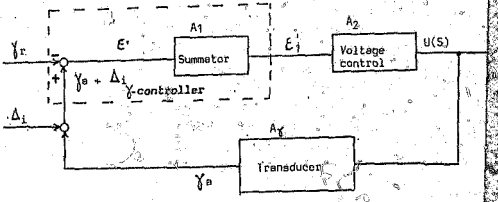


Fig. 4.7 γ Control loop block diagram. Disturbance at transducer output.

(c) Disturbances at the output of the Transducer

The disturbance Δ_i considered as voltage at the transducer output, may affect the control loop by adding a positive or negative quantity to the measured feedback value γ_a.* As experienced several times, if due to the disturbance effect γ_a decreases, (sometimes reaching zero) the error ε' will tend to γ_r, reaching zero) the error ε' will tend to γ_r, γ_r is negative. The valve firing will move towards the bigger angles, so as to decrease the bridge voltage and when $\gamma_a + \Delta_i = 0$, the firing angle of the valves is at the maximum value allowed for the γ extinction control loop. If Δ_i is not a transient disturbance, but is permanently present affecting the measurement of γ_a, the bridge voltage is also constantly affected and the deviation from its rated value can be considered proportional to Δ_i within the controlled angle range. For instance when $\gamma_a + \Delta_i = 0$, the bridge voltage drops to the minimum value Udicos(18°+$\Delta\gamma$) where $\Delta\gamma$ represents the γ deviation for $\Delta_i = -|\gamma_a|$. When Δ_i is a positive quantity (less probable), it modifies the γ_a in such a way that ε_1' increases towards zero. But deviations of ε_1' in that case can reach a maximum which depends on the minimum γ angle permitted. If ε_1' were not limited, it might rise to a value (+ 0,36 V), so that the γ extinction control loop is blocked from valve firing by the intervention of the minimum selecting circuit. Valve firing control is then taken by the inverter id controller, which

* γ_a = actual value of γ.

maintains a fixed output value (- 1,7 V) provided the system current *does not decrease*. Thus in case of a persistent controller outage, due to the presence of a steady disturbance, the Id controller performs the only possible *firing control*. The *firing of* the valves therefore is dictated by an open control loop, which does not assure the stability of the firing and does not react to bridge voltage variations.

If we consider now the transfer function of block diagram of fig. 4.7 with the only influence of disturbance at the transducer *output* it is *possible* to write:

$$U(s) = \frac{-A_L}{1-A} \cdot \gamma + \frac{A_L}{1-A} \cdot \Delta_3 = \frac{A_L}{1-A} \cdot (-\gamma + \Delta_3)$$

where $A = A_\gamma \cdot A_1 \cdot A_2$ and $A_L = A_1 \cdot A_2$

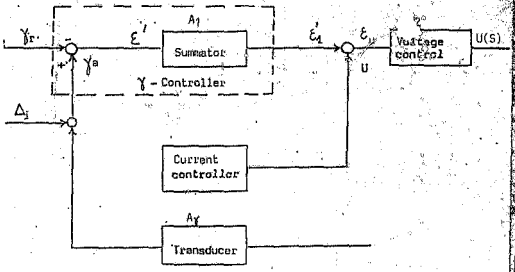


Fig. 4.8 Current controller controls firing when $\varepsilon' = (\gamma_n + \Delta_1) - \gamma_r) \geq 1{,}7V$ and also when $Id \leq 360A$.

Considering $A_1/(1 - A)$ as a constant, from the above relationship, it is possible to see that the output U(S) is varying linearly as a function of the disturbance Δ_i. In agreement with that stated before, we can therefore conclude:

$U(S) \rightarrow 0$ for $\Delta_i \rightarrow \gamma$

$U(S) \rightarrow$ the maximum value permitted for $\Delta_i \rightarrow -\gamma$
U(S) may represent the firing angle β.

(d) Disturbances on the Loop Direct Line

We now consider the γ control loop with the presence of a disturbance on the direct line, for instance, at the voltage control block input, (see Fig. 4.9).

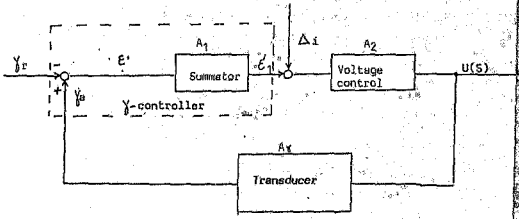


Fig. 4.9 γ Control loop block diagram, Disturbance at the γ controller output.

$U(S) = (\mathcal{E}_1' + \Delta_i) \cdot A_1 \cdot A_2 = A \cdot (\mathcal{E}_1' + \Delta_i)$
where $A = A_1 \cdot A_2$
Since $\mathcal{E}_1' = A_1 \cdot \mathcal{E}'$ we can re-write
$U(S) = A \cdot (A_1 \cdot \mathcal{E}' + \Delta_i)$. Therefore the error $\mathcal{E}' = \gamma_0 - \gamma_r$ can be also expressed as

$$\mathcal{E}' = -\gamma_r / (1 + A \cdot A_\gamma \cdot A_1) + \Delta_i \cdot A \cdot A_\gamma / (1 - A \cdot A_\gamma \cdot A_1)$$

Such a disturbance may effect the firing of the valves very badly, and can cause the inverter bridge to work under abnormal firing. It is possible, for instance, that the firing angle moves into the rectifier range of angles (0° to 90°) with a consequent reversal of DC voltage polarity across the bridge. This would lead to instability of the system, originating harmonics on DC links, and also, in the worst case, causing load rejection with the tripping of filters and generators at the rectifier station. Due to feedback action, the disturbances located at the loop forward path, cause the error $\mathcal{E}_1'$ to assume the extreme values permitted ($\mathcal{E}_1'$ max = - 1,7 V, $\mathcal{E}_1'$ min = - 3,6 V), at the γ controller output.

As a consequence, in a very short time after the occurance of Δ_i, one of two possibilities will arise:

(i) $U(S)$ min + ($\mathcal{E}_1'$max + Δ_i) when $\Delta_i > 0$
(ii) $U(S)$ max + ($\mathcal{E}_1'$min + Δ_i) when $\Delta_i < 0$

The equation (ii) gives β angle as the sum of the maximum firing angle permitted by the

Author Francocci Enrico
Name of thesis Automatic Control For A Hvdc Transmission Scheme. 1986

PUBLISHER:
University of the Witwatersrand, Johannesburg
©2013

LEGAL NOTICES:

Copyright Notice: All materials on the University of the Witwatersrand, Johannesburg Library website are protected by South African copyright law and may not be distributed, transmitted, displayed, or otherwise published in any format, without the prior written permission of the copyright owner.

Disclaimer and Terms of Use: Provided that you maintain all copyright and other notices contained therein, you may download material (one machine readable copy and one print copy per page) for your personal and/or educational non-commercial use only.

The University of the Witwatersrand, Johannesburg, is not responsible for any errors or omissions and excludes any and all liability for any errors in or omissions from the information on the Library website.